



**HAL**  
open science

## Nitroxide-mediated polymerization-induced self-assembly of amphiphilic block copolymers with a pH/temperature dual sensitive stabilizer block

X. Qiao, Pierre-Yves Dugas, Bernadette Charleux, Muriel Lansalot, Elodie Bourgeat-Lami

### ► To cite this version:

X. Qiao, Pierre-Yves Dugas, Bernadette Charleux, Muriel Lansalot, Elodie Bourgeat-Lami. Nitroxide-mediated polymerization-induced self-assembly of amphiphilic block copolymers with a pH/temperature dual sensitive stabilizer block. *Polymer Chemistry*, 2017, 8 (27), pp.4014 - 4029. 10.1039/c7py00595d . hal-01716126

**HAL Id: hal-01716126**

**<https://hal.science/hal-01716126>**

Submitted on 7 Oct 2021

**HAL** is a multi-disciplinary open access archive for the deposit and dissemination of scientific research documents, whether they are published or not. The documents may come from teaching and research institutions in France or abroad, or from public or private research centers.

L'archive ouverte pluridisciplinaire **HAL**, est destinée au dépôt et à la diffusion de documents scientifiques de niveau recherche, publiés ou non, émanant des établissements d'enseignement et de recherche français ou étrangers, des laboratoires publics ou privés.

# Nitroxide-mediated polymerization-induced self-assembly of amphiphilic block copolymers with a pH/temperature dual sensitive stabilizer block

X. G. Qiao,<sup>1,2</sup> P-Y. Dugas,<sup>1</sup> B. Charleux,<sup>1</sup> M. Lansalot,<sup>1</sup> E. Bourgeat-Lami<sup>1\*</sup>

<sup>1</sup> Univ Lyon, Université Claude Bernard Lyon 1, CPE Lyon, CNRS, UMR 5265, Chemistry, Catalysis, Polymers and Processes (C2P2), 43 Bvd. du 11 Nov. 1918, F-69616 Villeurbanne, France. <sup>2</sup> College of Chemistry and Chemical Engineering, and Henan Key laboratory of Function-Oriented Porous Materials, Luoyang Normal University, Luoyang 471934, China.

**ABSTRACT.** Comb-like terpolymers with a polymethacrylate backbone, carrying short pendant poly(ethylene)oxide (PEO) side chains ( $M_n = 300 \text{ g mol}^{-1}$ , 5 EO units), carboxylic acid groups and a few styrene (S) units [P(PEOMA<sub>300-co</sub>-MAA-co-S)-SG1], were synthesized by nitroxide-mediated polymerization, and used to initiate the emulsion polymerization of *n*-butyl methacrylate and styrene at 85 °C. The macroalkoxyamine initiators were shown to display a pH/temperature double responsive behavior. Above pH 5.7, the incorporation of MAA units in the copolymers shifted the solubility transition to higher temperatures whereas below pH 5.7, the cloud points decreased with increasing MAA content due to increased hydrophobicity of non-ionized MAA units and also possibly because of inter- or intrapolymeric H-bonding between the carboxylic acid groups of MAA and the oxygen atoms of PEO. Chain extension of the comb-like terpolymers with an immiscible poly(*n*-butyl methacrylate-co-styrene) block, carried out above or below the lower critical solution temperature (LCST) of the macroinitiator, resulted in electrosterically self-stabilized nano-objects with spherical, worm-like or vesicular nanostructures. The effect of the composition of the hydrophilic block, the pH and the macroinitiator concentration on the control of the polymerization, the polymerization kinetics and the particle morphology was studied in details. Compared to their P(PEOMA<sub>300-co</sub>-S)-SG1 or P(PEOMA<sub>950-co</sub>-S)-SG1 homologues, the macroalkoxyamine terpolymers displayed significantly different stabilizing properties which directly influenced the phase diagram. At last, hybrid nanostructures consisting of silica particles decorated by self-assembled block copolymers were also reported using the macroalkoxyamine initiator containing 14 mol% of MAA. Interestingly, the polymerization performed at pH 9 resulted in partially coalesced short worms radially expanding from the silica core in a sea urchin-like morphology.

**Keywords:** block copolymers, thermo- and pH-responsive, emulsion polymerization, PISA, morphology, silica.

## INTRODUCTION

Polymerization-induced self-assembly (PISA) has recently emerged as a method of choice for the synthesis of self-stabilized nano-objects in aqueous emulsion.<sup>1,2,3</sup> Initially developed to circumvent the difficulties inherent to the implementation of reversible deactivation radical polymerization (RDRP) processes in dispersed media,<sup>4</sup> PISA has gradually evolved towards a very efficient and versatile technique for the production of block copolymer nanoparticles without resorting to the use of toxic co-solvents.<sup>2,5</sup> Not only can such particles be obtained at relatively high solids contents in purely aqueous solution, but their size, surface functionality and morphology can also be finely tuned by careful monitoring of the architecture and molar mass of the hydrophilic and hydrophobic blocks, giving this technique considerable potential for the elaboration of new materials such as Pickering emulsifiers,<sup>6,7</sup> nanostructured films,<sup>8</sup> thermoresponsive nanogels,<sup>1</sup> drug delivery vehicles or organic/inorganic hybrids.<sup>5,9,10</sup> Alongside the development of new products and applications, a substantial amount of work has been done over the past ten years in an effort to rationalize the parameters that determine the morphologies obtained by PISA.<sup>1,3</sup> It is now admitted that particle morphologies are primarily dictated by the relative volume fraction of the two blocks, which in turns depends on their respective degrees of polymerization, as described by the packing parameter.<sup>11,12</sup> Hence, various authors have reported a gradual change of particle morphology from spheres to worms to vesicles upon increasing the molar mass of the hydrophobic block either during the course of the polymerization, or at full conversion by decreasing the control agent concentration. Varying the chemical composition, the length<sup>13</sup> or the topology<sup>14</sup> of the hydrophilic block was also shown to significantly influence particle morphology.<sup>1,2</sup> Actually, any parameter that can influence the degree of solvation and conformation of the hydrophilic block can potentially have an impact on the self-assembly process. Most studies in this area

have been performed using the reversible addition-fragmentation chain transfer (RAFT) technique. For instance, Boissé *et al.*<sup>15</sup> reported the first example of non-spherical morphologies obtained by RAFT emulsion polymerization of styrene using a pH-sensitive hydrophilic block composed of acrylic acid (AA) and poly(ethylene oxide) methyl ether acrylate (PEOA). Decreasing the ionization degree of AA (at low pH) or increasing the salt concentration (at high pH) - which both influenced the water solubility of the macroRAFT agent - favored the formation of fibers and vesicles in a similar way as reported earlier by Zhang and Eisenberg<sup>16</sup> during the post-polymerization self-assembly of polystyrene-*b*-poly(acrylic acid) diblock copolymers. The effect of ionic strength on the morphology of self-assembled block copolymers was also recently reported by our group during nitroxide-mediated emulsion polymerization of *n*-butyl methacrylate (BMA) with a small amount of styrene (S) initiated by a PEO-based macroalkoxyamine.<sup>17</sup> Various authors have also employed the temperature to trigger morphological transitions of particles obtained by PISA. For instance, Armes and co-workers showed that poly(glycerol mono methacrylate)-*b*-poly(2-hydroxypropyl methacrylate)<sup>19</sup> or poly(ethylene oxide)-*b*-poly(2-hydroxypropyl methacrylate)<sup>20</sup> diblock copolymer assemblies can exhibit respectively worm-to-sphere or vesicle-to-sphere reorganizations, after cooling below a certain temperature which depends on the copolymer composition. It was shown recently that order-order transitions can also be triggered by a change of pH<sup>21,22</sup> or a change of both pH and temperature.<sup>23</sup> However, less attention has been paid to self-assembly processes in which a change of particle morphology can be induced by a change of temperature in the course of the polymerization. Recently, Figg *et al.*<sup>24</sup> reported a new concept, called polymerization-induced thermal self-assembly, wherein chain extension was performed above the lower critical solution temperature (LCST) of the hydrophobic block. The latter thus underwent a thermally triggered soluble-insoluble phase transition and self-assembled into vesicles or short worms, which were subsequently

frozen by crosslinking. It is worth mentioning that a similar strategy was previously reported by Delaittre *et al.*<sup>25</sup> for the synthesis of crosslinked thermoresponsive poly(*N,N*-diethylacrylamide) nanogel particles which displayed a reversible swelling/deswelling transition around 32 °C. In the same vein, there are also two recent examples involving a thermoresponsive “stabilizer” block in RAFT emulsion polymerization.<sup>26,27</sup> However, as the polymerization was carried out above their LCST, the thermoresponsive polymers could no longer act as stabilizers, and a surfactant was necessary to stabilize the resulting assemblies. These examples cannot therefore really be considered to follow the conventional PISA mechanism.

To the best of our knowledge, there is as yet no example of a PISA system involving the use of a hydrophilic block that is responsive to both pH and temperature. Indeed, as mentioned previously, using a stabilizer block that undergoes a volume phase transition during the course of the polymerization may result in stability issues. However, we thought that dual sensitive polymers, *i.e.* thermoresponsive polymers that could also respond to a change of pH, could afford stable systems as long as the pH is kept at a minimum value to avoid complete phase separation of the stabilizing block in order to preserve the colloidal stability of the resulting assemblies.

In the present work, we report the SG1-mediated synthesis of comb-like macroalkoxyamine initiators composed of poly(ethylene oxide) methyl ether methacrylate (PEOMA<sub>300</sub>), methacrylic acid (MAA) and S units. These terpolymers exhibit a dual pH/temperature responsive behavior induced by the incorporation of MAA units. Emulsion copolymerization of BMA and S carried out below or above the LCST of the macroalkoxyamine initiators resulted in different self-assembled polymeric nanoparticle morphologies, which were function of the suspension pH, the composition of the hydrophilic block and the macroinitiator concentration. We showed that the temperature and pH dual-responsive

behavior of the macroinitiators was directly reflected in the final particle morphology. In a last part, the dual stimuli-responsive behavior of the terpolymers was also briefly exploited to synthesize polymer/silica composite particles relying on the well-known affinity of PEO for silica surfaces.

## EXPERIMENTAL SECTION

**Materials.** The *N*-tert-butyl-*N*-(1-diethyl phosphono-2,2-dimethylpropyl) nitroxide (SG1, 85%) and *N*-(2-methylpropyl)-*N*-(1-diethylphosphono-2,2-dimethylpropyl)-*O*-(2-carboxyl prop-2-yl) alkoxyamine initiator (BlocBuilder<sup>®</sup>, 99%) were kindly supplied by Arkema. The monomers: styrene (S, 99%, Acros) and methacrylic acid (MAA, 99%, Aldrich), and the macromonomer: poly(ethylene oxide) methyl ether methacrylate (PEOMA<sub>300</sub>, number-average molar mass  $M_n = 300 \text{ g mol}^{-1}$ , Aldrich) were used without further purification. Dimethyl sulfoxide (DMSO, Aldrich), diethyl ether (Acros Organics), hydrochloric acid (HCl, Sigma-Aldrich, 0.1 N) and sodium hydroxide (NaOH, SDS, 0.1 M solution in water) were used as received. The commercial silica sol (Klebosol 30N50) was kindly supplied by Clariant (France). Deionized water (Purelab Classic UV, ElgaLabWater) was used for all experiments.

**Synthesis of comb-like P(PEOMA<sub>300</sub>-*co*-MAA-*co*-S)-SG1 macroinitiators.** The terpolymer macroinitiators were synthesized following a protocol similar to the one reported previously for P(PEOMA-*co*-S)-SG1 copolymers<sup>17</sup> with slight modifications (see Supporting Information for the detailed procedure). A kinetic analysis was first carried out under the conditions given in Table 1, and the polymerizations were then reproduced on a larger scale in a 500 mL three-neck round-bottom flask to get a larger amount of polymer to be used as macroinitiator in emulsion polymerization experiments. The polymerizations were stopped

after 1 h, and the final products were dried under vacuum after precipitation in diethyl ether before analysis. Their characteristics are shown in Table 2.

**Table 1.** Experimental conditions for the SG1-mediated copolymerization of PEOMA, MAA and S initiated by the BlocBuilder<sup>®</sup> alkoxyamine in DMSO at 80 °C (monomer concentration = 30 wt%; initial molar fraction of free SG1 versus BlocBuilder<sup>®</sup>:  $r = 0.119$ ).

Run	[PEOMA <sub>300</sub> ] (mol L <sup>-1</sup> )	[MAA] (mol L <sup>-1</sup> )	[S] (mol L <sup>-1</sup> )	[SG1] <sub>0</sub> (mol L <sup>-1</sup> )	[BlocBuilder <sup>®</sup> ] (mol L <sup>-1</sup> )	$f_{0,S}$ <sup>a</sup>	Target $M_n$ (g mol <sup>-1</sup> ) <sup>b</sup>
<b>M0</b>	0.83	0	0.080	0.001	0.0087	0.088	29 930
<b>M1</b>	1.08	0.27	0.16	0.0015	0.014	0.105	26 030
<b>M2</b>	0.71	0.77	0.17	0.0017	0.015	0.103	19 560
<b>M3</b>	0.34	1.35	0.18	0.0020	0.015	0.096	14 610

<sup>a</sup> Initial molar fraction of styrene. <sup>b</sup> Theoretical molar mass at 100% conversion determined according to:  $\text{Target } M_n (\text{g mol}^{-1}) = MW^{\text{BlocBuilder}^{\text{®}}} + \left( \frac{\text{initial mas of monomer}}{\text{mass of BlocBuilder}^{\text{®}}} \right) \times MW^{\text{BlocBuilder}^{\text{®}}}$ .

**Table 2.** Main characteristics of the macroalkoxyamine initiators synthesized in this work on a larger scale, following the experimental conditions shown in Table 1, for their use as initiators in emulsion polymerization.<sup>a</sup>

Run	Target $M_n$ (g mol <sup>-1</sup> ) <sup>b</sup>	Overall molar conv. (%)	$M_n$ <sup>c</sup> (g mol <sup>-1</sup> )	$D$ <sup>c</sup>	Structure of the copolymers
<b>Ma0</b>	29 920	33.2	12 100	1.17	P[(PEOMA <sub>300</sub> ) <sub>38</sub> -CO-S <sub>3</sub> ]
<b>Ma1</b>	26 000	43.4	11 600	1.37	P[(PEOMA <sub>300</sub> ) <sub>34</sub> -CO-MAA <sub>6.7</sub> -CO-S <sub>7.2</sub> ]
<b>Ma2</b>	19 600	57.4	11 800	1.40	P[(PEOMA <sub>300</sub> ) <sub>29</sub> -CO-MAA <sub>26</sub> -CO-S <sub>7.3</sub> ]
<b>Ma3</b>	14 600	55.0	8 500	1.32	P[(PEOMA <sub>300</sub> ) <sub>13</sub> -CO-MAA <sub>44</sub> -CO-S <sub>8</sub> ]

<sup>a</sup> Reaction time = 1 h. T = 80 °C. <sup>b</sup> Theoretical molar mass at 100% conversion determined according to:  $\text{Target } M_n (\text{g mol}^{-1}) = MW^{\text{BlocBuilder}^{\text{®}}} + \left( \frac{\text{initial mas of monomer}}{\text{mass of BlocBuilder}^{\text{®}}} \right) \times MW^{\text{BlocBuilder}^{\text{®}}}$ .

<sup>c</sup> Experimental  $M_n$  and dispersity determined by SEC in THF using PMMA calibration.

**Surfactant-free emulsion polymerizations.** The surfactant-free emulsion copolymerization of BMA with a small percentage of styrene was carried out at 85 °C. In a typical experiment (E2 in Table 3), a known quantity of macroinitiator (Ma1, 0.99 g; 0.0052 mol L<sup>-1</sup>) was firstly

dissolved in 12.5 g water and the obtained solution was stirred under nitrogen bubbling for 30 min in an ice bath. Then, the monomers, BMA and styrene (2.35 g of BMA and 0.15 g of S), were added into the aqueous solution. The resulting mixture was deoxygenated by nitrogen bubbling for another 20 min, introduced into a 50 mL round-bottom flask and heated at 85 °C for at least 2 h. Time zero of the polymerization was taken when the reaction temperature reached 75 °C. Samples were periodically withdrawn to follow monomer conversion by gravimetric analyses. The pH of the solutions were carefully adjusted by adding a few drops of sodium hydroxide (NaOH, 0.1 M aqueous solution) before introducing the monomers. The experimental conditions for the polymerizations performed in this study are displayed in Table 3.

**Surfactant-free emulsion polymerizations in the presence of silica particles.** In a typical experiment (entry ES01 in Table 4), a known quantity of macroinitiator (Ma1, 0.88 g; 2.3 mmol L<sup>-1</sup>) was first dissolved in the silica suspension (25 g, Klebosol 30N50,  $D_{n\text{ TEM}} = 77$  nm, [SiO<sub>2</sub>] = 50 g L<sup>-1</sup>). A 1 M NaOH standard solution was used to adjust the pH value and the mixture was then stirred under nitrogen bubbling for 30 min at room temperature. Then, the monomers, a mixture of BMA (2.35 g) and S (0.15 g), were introduced in the suspension and the obtained system was deoxygenated by nitrogen bubbling for another 20 min, and finally transferred into a 50 mL round bottom flask. The mixture was then heated at 85 °C for 6 h. Samples were periodically withdrawn to follow monomer conversion by gravimetric analysis. The experimental conditions and main characteristics of the resulting latex particles are listed in Table 4.

**Table 3.** Recipes and main characteristics of the polymer latex particles synthesized by surfactant-free emulsion polymerization of *n*-butyl methacrylate with a low percentage of styrene using SG1-capped P(PEOMA<sub>300</sub>-*co*-MAA-*co*-S) copolymers as macroinitiators. Effect of the nature and concentration of macroinitiator and the pH.<sup>a</sup>

Entry	Macroinitiator type	(mmol L <sup>-1</sup> )	Target $M_n$ (g mol <sup>-1</sup> ) <sup>b</sup>	pH <sup>c</sup>	Cloud point (°C) <sup>d</sup>	$X_{wt}$ (%) <sup>e</sup>	$M_n$ (Đ) <sup>f</sup>	Particle morphology <sup>g</sup>	$D_n^h$ (nm)	$D_w/D_n^h$ (TEM)	[NaOH] (mol L <sup>-1</sup> ) <sup>i</sup>
E1	Ma1	2.6	75 090	7.5	/	71.3	87 900 (1.95)	v (+ s)	/	/	$1.7 \times 10^{-2}$
E2	Ma1	5.2	43 260	7.5	/	78.2	55 700 (2.17)	f + v	59	1.32	$3.5 \times 10^{-2}$
E3	Ma1	9.1	29 790	7.5	/	88.7	45 500 (2.16)	s + f	/	/	$6.0 \times 10^{-2}$
E4	Ma2	5.3	41 740	5.0	34	52.5	27 300 (1.91)	Mainly v	/	/	/
E5	Ma2	5.5	42 160	6.0	67	60.7	36 600 (1.90)	f + v	/	/	$3.2 \times 10^{-2}$
E6	Ma2	5.4	42 130	7.5	/	54.0	38 700 (1.99)	s	78	1.09	$5.1 \times 10^{-2}$
E7	Ma2	5.4	42 230	9.1	/	48.6	30 600 (2.08)	s	70	1.07	$5.4 \times 10^{-2}$
E8	Ma3	5.1	41 480	7.5	/	40.8	44 100 (1.77)	s (+ f + v)	108	1.06	$6.4 \times 10^{-2}$

<sup>a</sup> All polymerizations were carried out at 85 °C for at least 2 h. The total monomer concentration was 20 wt% and the initial molar fraction of styrene was  $f_{S0} = 0.08$ .

<sup>b</sup> Theoretical molar mass at 100% conversion determined according to:  $\text{Target } M_n (\text{g mol}^{-1}) = MW^{\text{macroinitiator}} + \left( \frac{\text{initial mas of monomer}}{\text{mass of macroinitiator}} \right) \times MW^{\text{macroinitiator}}$ .

<sup>c</sup> Initial pH determined before polymerization. <sup>d</sup> Determined by UV/Vis spectroscopy (see characterization part). <sup>e</sup> Weight conversion determined by gravimetric analysis. <sup>f</sup> Determined by SEC in THF using PMMA standards. <sup>g</sup> s = spheres, f = fibers and v = vesicles, <sup>h</sup> Number-average diameter and polydispersity index of the spherical particles as determined by TEM analysis. <sup>i</sup> Determined from the amount of 1 M NaOH solution added at the beginning of the polymerization.

**Table 4.** Experimental conditions and characteristics of the silica/polymer latex particles synthesized by surfactant-free emulsion polymerization of *n*-butyl methacrylate and styrene using Ma1 (see Table 2) as macroinitiator in the presence of 77 nm diameter silica particles for different pH values.<sup>a</sup>

Entry	pH <sup>b</sup>	[Macroinitiator] (mmol L <sup>-1</sup> )	Target $M_n$ (g mol <sup>-1</sup> ) <sup>c</sup>	Conv. (%) <sup>d</sup>	$M_n$ (Đ) <sup>e</sup>	Composite particle morphology
ES01	6.0	5.2	43 200	57	52 200 (1.93)	Dumbbells, snowman vesicles
ES02	7.5	5.2	43 600	59	52 000 (2.15)	Multipod-like
ES03	9.0	5.2	43 500	61	49 300 (2.18)	Sea urchin-like

<sup>a</sup> All polymerizations were carried out at 85 °C for 6 h with [SiO<sub>2</sub>] = 50 g L<sup>-1</sup>. The total monomer concentration was 20 wt% and the initial molar fraction of styrene was  $f_{S0} = 0.08$ . <sup>b</sup> Initial pH determined before polymerization. <sup>c</sup> Theoretical molar mass at 100% conversion determined according to: Target  $M_n$  (g mol<sup>-1</sup>) =  $MW^{macroinitiator} + \left(\frac{\text{initial mas of monomer}}{\text{mass of macroinitiator}}\right) \times MW^{macroinitiator}$ .

<sup>d</sup> Determined by gravimetric analysis. <sup>e</sup> Determined by SEC in THF with PMMA standards.

**Characterizations.** The polymerization kinetics was monitored by <sup>1</sup>H NMR spectroscopy. The analyses were performed in 5 mm diameter tubes in DMSO-d<sub>6</sub> at room temperature (Bruker DRX 300). The individual molar conversions of S, PEOMA and MAA ( $X_S$ ,  $X_{PEOMA}$  and  $X_{MAA}$ , respectively) during the macroinitiator synthesis were determined by measuring the vinyl proton integrals of the monomers (three vinyl protons of S at  $\delta = 6.74$  ppm,  $\delta = 5.83$  ppm and  $\delta = 5.25$  ppm, two CH<sub>2</sub> protons at  $\delta = 6.04$  ppm and  $\delta = 5.69$  ppm for PEOMA and two vinyl protons at 5.84 and 5.29 ppm for MAA) using 1,3,5-trioxane as an internal reference ( $\delta = 5.12$  ppm). The chemical shift scale was calibrated relative to tetramethylsilane. The overall conversion considered was the molar conversion,  $X_{mol}$ , directly accessible via the NMR analysis and calculated from the individual monomer conversions according to the relationship:  $X_{mol} = X_S \times f_{S,0} + X_{PEOMA} \times f_{PEOMA,0} + X_{MAA} \times f_{MAA,0}$  where  $f_{S,0}$ ,  $f_{PEOMA,0}$  and  $f_{MAA,0}$  are, respectively, the initial molar fractions of S, PEOMA and MAA in the monomer mixture. For the plots representing  $M_n$  as a function of the overall conversion, the weight conversion was used, and calculated according to  $X_{wt} = X_S \times W_{S,0} + X_{PEOMA} \times W_{PEOMA,0} + X_{MAA} \times W_{MAA,0}$

where  $W_{S,0}$ ,  $W_{PEOMA,0}$  and  $W_{MAA,0}$  are, respectively, the initial weight fractions of S, PEOMA and MAA in the monomer mixture.

Size exclusion chromatography (SEC) analyses were performed in THF. All polymers were injected at a concentration of  $3 \text{ mg mL}^{-1}$  after filtration through a  $0.45 \text{ }\mu\text{m}$  pore-size membrane. The separation was carried out on three Polymer Laboratories columns [ $3 \times$  PLgel  $5 \text{ }\mu\text{m}$  Mixed C ( $300 \times 7.5 \text{ mm}$ )] and a guard column (PL gel  $5 \text{ }\mu\text{m}$ ). Columns and detectors were maintained at  $40 \text{ }^\circ\text{C}$ . THF was used as the mobile phase at a flow rate of  $1 \text{ mL min}^{-1}$  and toluene served as a flow rate marker. The device (Viscotek TDA305) was equipped with a refractive index (RI) detector ( $\lambda = 670 \text{ nm}$ ). The number-average molar mass ( $M_n$ ) and dispersity ( $D = M_w/M_n$ , with  $M_w$ : weight-average molar mass) were derived from the RI signal by a calibration curve based on poly(methyl methacrylate) standards (PMMA from Polymer Laboratories). Before analysis, the polymers were modified by methylation of the carboxylic acid groups using trimethylsilyl diazomethane as reported elsewhere.<sup>28</sup> Samples synthesized in the presence of silica were first dried at room temperature for 2 days and then diluted in THF (THF for HPLC) under stirring. The solution was then centrifuged at  $21\ 000 \text{ rpm}$  for 1 h to remove the silica particles and the recovered polymer chains were methylated as described above before injection.

The cloud points of the macroinitiator solutions in water were determined by monitoring the transmittance at  $500 \text{ nm}$  as a function of temperature using a Shimadzu (UV-1800) UV-visible (UV-Vis) spectrometer. The temperature range was from  $20$  to  $80 \text{ }^\circ\text{C}$  and the heating rate was  $1 \text{ }^\circ\text{C min}^{-1}$ .

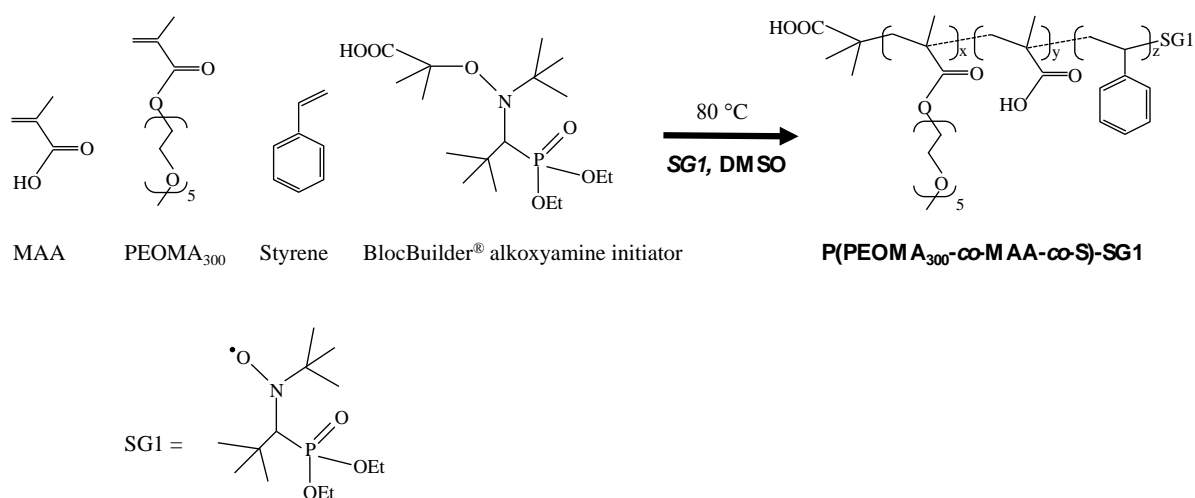
Transmission electron microscopy (TEM) was performed at an accelerating voltage of  $80 \text{ kV}$  with a Philips CM120 transmission electron microscope (Centre Technologique des Microstructures, platform of the Université Claude Bernard, Lyon 1). Highly diluted samples were dropped on a formvar-carbon coated copper grid and dried under air. Phosphotungstic

acid (1.5 wt%, pH = 7) was used to increase the specimen contrast. For the cryo-transmission electron microscopy (cryo-TEM) analysis, the diluted samples were dropped onto 300 Mesh holey carbon films (Quantifoil R2/1) and quench-frozen in liquid ethane using a cryo-plunge workstation (made at LPS Orsay). The specimens were then mounted on a precooled Gatan 626 specimen holder, transferred in the microscope (Phillips CM120) and observed at an accelerating voltage of 120 kV. The number-average ( $D_n$ ) and the weight-average particle diameter ( $D_w$ ), and the polydispersity index ( $PDI = D_w/D_n$ ) of the spherical particles were calculated using  $D_n = \sum n_i D_i / \sum n_i$  and  $D_w = \sum n_i D_i^4 / \sum n_i D_i^3$ , where  $n_i$  is the number of particles with diameter  $D_i$ .

## RESULTS AND DISCUSSION

### 1. Synthesis of comb-like P(PEOMA-*co*-MAA-*co*-S)-SG1 macroalkoxyamine initiators

Synthesis of the comb-like P(PEOMA-*co*-MAA-*co*-S)-SG1 macroalkoxyamine initiators was carried out under mild conditions in DMSO solution at 80 °C, using BlocBuilder® as an alkoxyamine initiator in the presence of approximately 10 mol% of styrene as depicted in Scheme 1. Table 1 gives the experimental conditions of three different reactions, for which the polymerization kinetics was followed carefully. To allow for a faithful comparison between all P(PEOMA<sub>300</sub>-*co*-MAA-*co*-S)-SG1 terpolymers, we fixed their targeted number-average degrees of polymerization around 110, and only varied the PEOMA<sub>300</sub> to MAA ratio. The individual S, MAA and PEOMA<sub>300</sub> molar conversions were determined by <sup>1</sup>H NMR as described in the experimental section. Figure 1 shows the evolution of both individual and overall monomer conversions with time for the three comonomer compositions.



**Scheme 1.** Scheme illustrating the synthesis of comb-like P(PeOMA<sub>300</sub>-co-MAA-co-S)-SG1 macroalkoxyamine initiators using BlocBuilder<sup>®</sup> as alkoxyamine initiator in DMSO at 80 °C in the presence of a small amount of free SG1 nitroxide.

In all cases, conversions higher than 70% were obtained in less than 3 hours. The kinetic plots clearly show that S was consumed faster than MAA or PEOMA, resulting in a composition drift with polymer chains initially richer in styrene units, especially for M1. Furthermore, the plots also indicate a higher conversion for PEOMA than for MAA. As seen in Figure 2a, the first-order kinetic plots are linear, accounting for a constant number of propagating radicals. The higher the MAA content, the lower were the slopes and the final conversions. Furthermore, the evolutions of  $M_n$  and  $D$  measured by SEC in THF as a function of the overall weight conversion show a linear increase and low molar mass distributions ( $D < 1.6$ ) (Figure 2b) indicating a good control of the polymerization. The controlled character of the polymerization was further attested by the complete shift of the SEC traces toward higher molar masses with increasing monomer conversion (Figure 3).

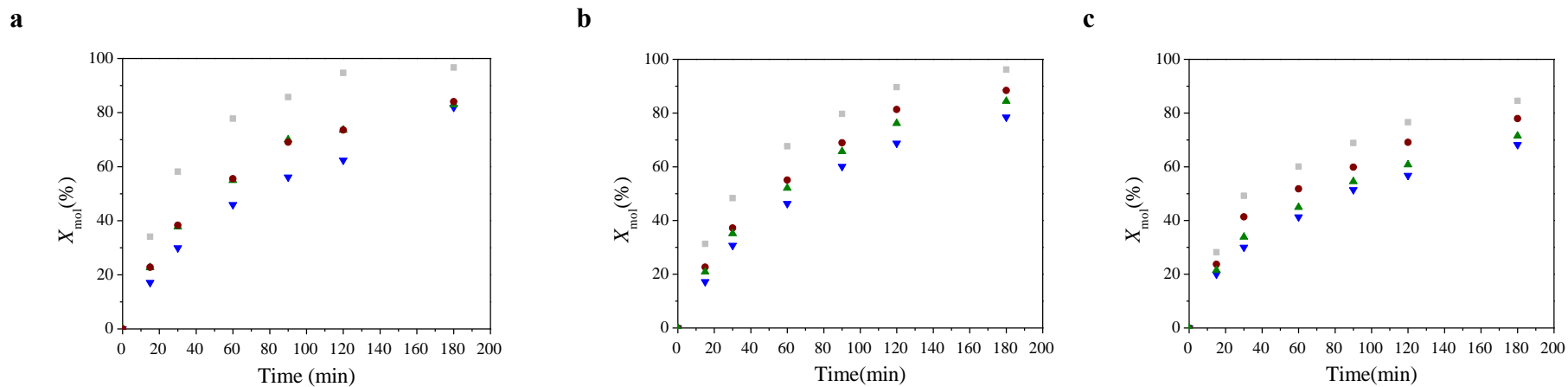


**Figure 1.** Molar conversion vs time plots (■: styrene, ● PEOMA<sub>300</sub>, ▼ MAA, ▲ Overall conversion) for the synthesis of P(PEOMA<sub>300</sub>-co-MAA-co-S)-SG1 macroinitiators with different molar ratios of PEOMA<sub>300</sub> and MAA: a) M1 (PEOMA<sub>300</sub>/MAA= 4/1), b) M2 (PEOMA<sub>300</sub>/MAA = 0.9/1), and c) M3 (PEOMA<sub>300</sub>/MAA = 1/4) (Table 1).

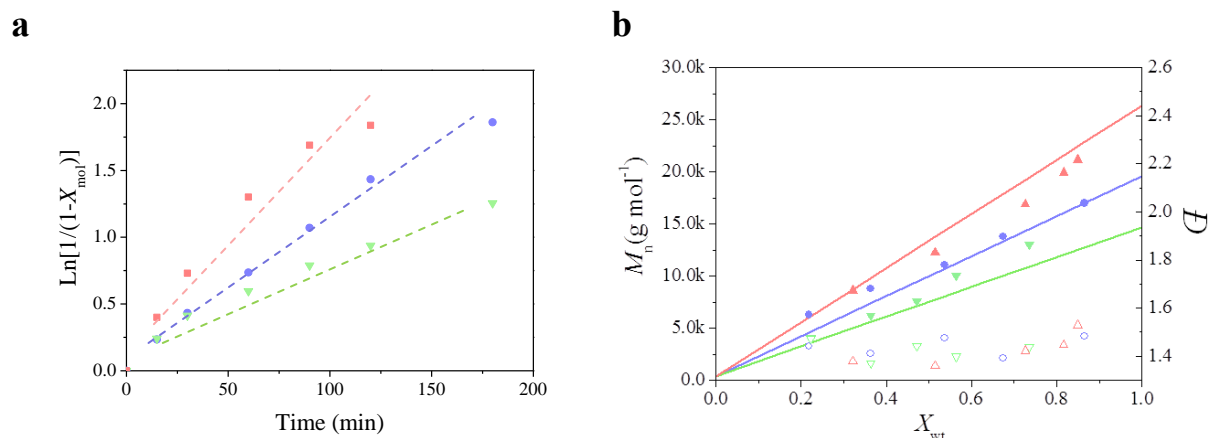


**Figure 2.** a)  $\text{Ln}[1/(1-X_{\text{mol.}})]$  vs time plots, and b) evolutions of  $M_n$  (filled symbols) and  $\bar{D}$  (empty symbols) with weight conversion during the synthesis of P(PEOMA<sub>300</sub>-co-MAA-co-S)-SG1 macroinitiators for varying PEOMA<sub>300</sub> to MAA molar ratios. M1 (PEOMA<sub>300</sub>/MAA = 4/1, ■), M2 (PEOMA<sub>300</sub>/MAA = 0.9/1, ●) and M3 (PEOMA<sub>300</sub>/MAA = 1/4, ▼) (Table 1). The straight lines in the  $M_n$  vs  $X_{\text{wt}}$  plots correspond to the theoretical evolution.

Due to the quality of the results obtained, the same experimental conditions were applied to target a larger amount of the three macroalkoxyamines, to be used as macroinitiators in the emulsion polymerization of BMA in presence of a small amount of S. As styrene was consumed faster than MAA and PEOMA, the polymerization was stopped at around 50 % conversion to avoid the formation of a too large proportion of dead chains by irreversible termination reactions and ensure the successful formation of block copolymers during the emulsion step. Indeed, as discussed earlier,<sup>29</sup> the presence of styrene is the key for an efficient control of the polymerization of methacrylic monomers. The results are summarized in Table 2, and show again a good control of the polymerization ( $\bar{D} < 1.4$ ). Using  $M_n$  from SEC (THF solvent with PMMA calibration) and the average composition of the copolymers (molar fractions) from NMR, it was possible to determine the average number of comonomer units within the chains as indicated in Table 2. After polymerization, the polymers were purified by precipitation in diethyl ether, to remove all traces of unreacted monomers.

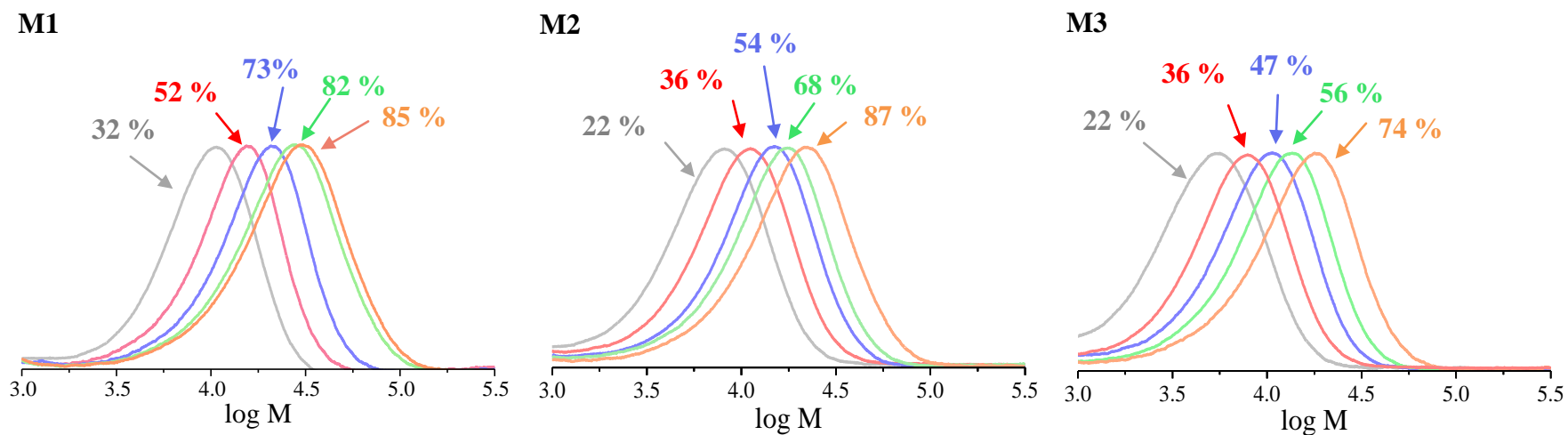


**Figure 3.** Evolution of the size exclusion chromatograms (SEC in THF, PMMA calibration) with weight conversion during the synthesis of P(PEOMA<sub>300</sub>-co-MAA-co-S)-SG1 macroinitiators for varying PEOMA<sub>300</sub> to MAA molar ratios. M1 (PEOMA<sub>300</sub>/MAA = 4/1), M2 (PEOMA<sub>300</sub>/MAA = 0.9/1) and M3 (PEOMA<sub>300</sub>/MAA = 1/4) (Table 1).

## **2. Effect of pH on the thermoresponsive behavior of the P(PEOMA<sub>300</sub>-*co*-MAA-*co*-S) terpolymers**

PEOMA-based polymers are well known to exhibit a thermoresponsive behavior in aqueous solution, characterized by a LCST-type phase transition which depends on the length of the PEO side-chains, and in the case of copolymers on the comonomer composition.<sup>30,31</sup> As reported in our previous work,<sup>17</sup> the PEOMA<sub>300</sub>-based macroalkoxyamine initiator (P[(PEOMA<sub>300</sub>)<sub>38</sub>-*co*-S<sub>3</sub>]-SG1, Ma0 in Table 2) has a cloud point of 51 °C at pH = 4, as determined by UV-Vis spectroscopy (Figure S1, Supporting Information). The light transmittance profile reflects a typical behavior of LCST-type phase separation, where solutions are 100% transparent at low temperature and quickly become cloudy (0% transmittance) above the critical temperature, illustrating the sudden solubility drop of the polymer in water. As Ma0 contains only one terminal methacrylic acid unit, its LCST is independent of pH in the range 4 to 8 (data not shown). In contrast, as shown in Figure 4, the solution pH had a strong influence on the cloud point of the P(PEOMA<sub>300</sub>-*co*-MAA-*co*-S) terpolymers. The transmittance curves of the macroalkoxyamine containing 14 mol% of MAA (Ma1, Table 2, Figure 4a) were gradually shifted to higher temperatures with increasing pH attesting for its dual pH/temperature stimuli-responsive behavior, while in parallel the phase transition became less sharp.

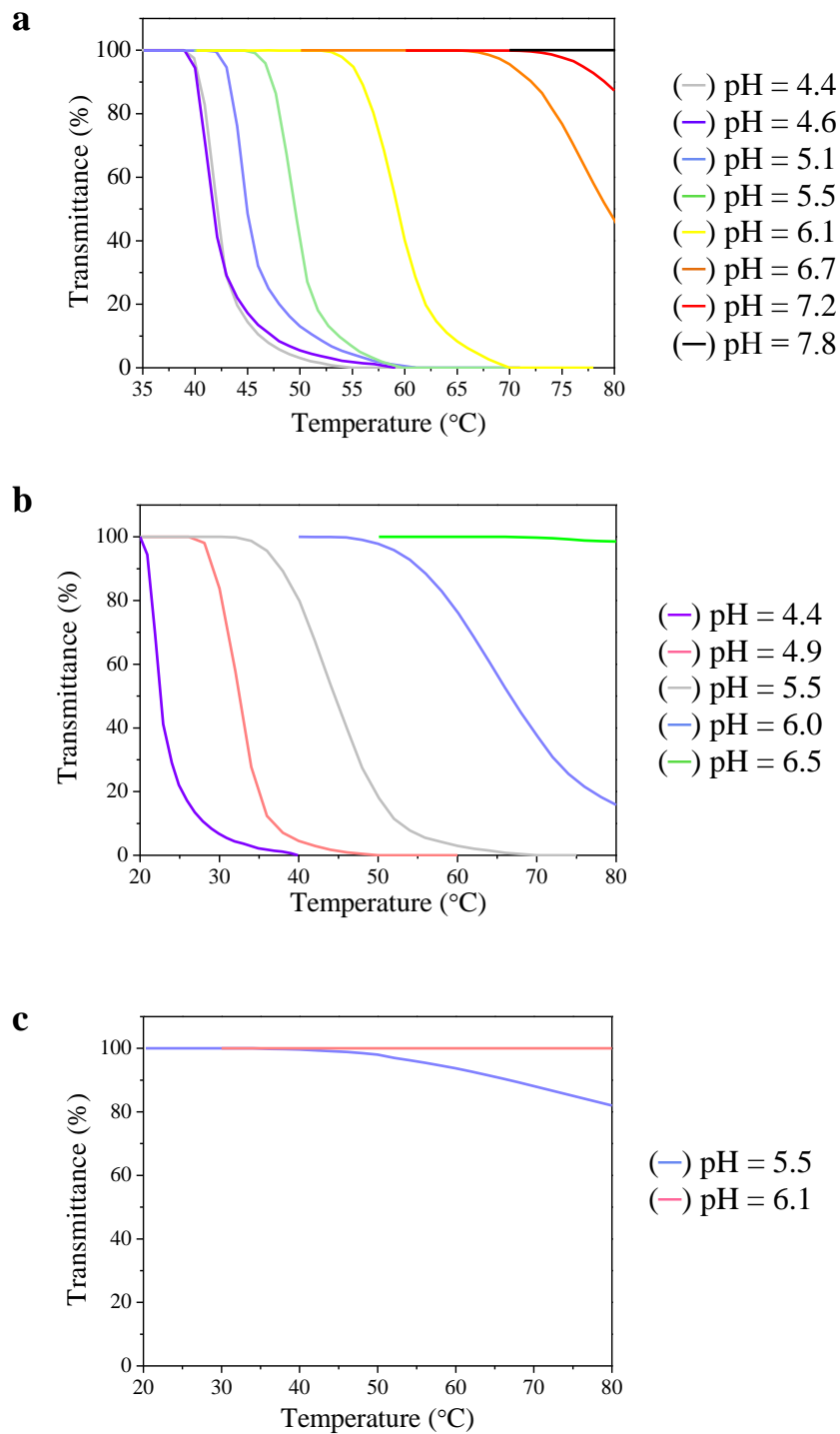


**Figure 4.** Plots of transmittance as a function of temperature (heating rate = 1 °C min<sup>-1</sup>) for aqueous solutions (0.5 wt%) of SG1-capped P(PeOMA<sub>300</sub>-co-MAA-co-S) macroinitiators: a) Ma1, b) Ma2 and c) Ma3 as measured by UV-Vis spectroscopy ( $\lambda = 500$  nm) for different pH values. See Table 2 for experimental details.

Similar results were observed for Ma2 (42 mol% of MAA, Figure 4b) and Ma3 (68 mol%, Figure 4c), for however a narrower range of pH values. Indeed, the water solubility of P(PEOMA<sub>300-co</sub>-MAA-co-S) macroinitiators increased with increasing MAA content at high pH values, whereas the MAA-rich terpolymer (Ma3, 68 mol% MAA) was fully insoluble below pH 4.9 (Figure S2, Supporting Information) in agreement with previous literature.<sup>32</sup> Ma2 was thus thermoresponsive between pH 4.5 and pH 6.0 while Ma3 appeared to be solely pH-responsive, even though Figure 4c indicates a slow decrease in transmittance around 43 °C at pH = 5.5. These results thus demonstrate that the LCST of the P(PEOMA<sub>300-co</sub>-MAA-co-S) terpolymers can be finely tuned over a broad range of temperatures around the cloud point of the P(PEOMA<sub>300-co</sub>-S) macroinitiator.

We have plotted in Figure 5 the evolution of the LCST of the Ma0, Ma1 and Ma2 macroalkoxyamine initiators as a function of pH. Interestingly, the three curves intersect at around pH 5.7. Indeed, for pH values higher than 5.7, the MAA units are likely deprotonated and the cloud point therefore increases as the hydrophilicity of the terpolymers increases. On the contrary, below pH 5.7, the cloud point decreases upon the incorporation of MAA units indicating decreased water solubility. Possible interpretations for this unexpected clouding behavior at low pH values are: i) the rather hydrophobic character of MAA and ii) the possible formation of intra or intermolecular interactions between the carboxylic acid groups of MAA and the ether oxygen groups of PEO leading to self-complexation as previously reported in the literature.<sup>33,34</sup> The LCST decreases as the degree of hydrophobicity increases consecutively to water expulsion from the hydration shell. Note that a similar dual responsive behavior has already been observed for P(PEOMA<sub>300-co</sub>-MAA) copolymers,<sup>32</sup> but it is, to our best knowledge, the first time that it is reported for P(PEOMA<sub>300-co</sub>-MAA-co-S) terpolymers.

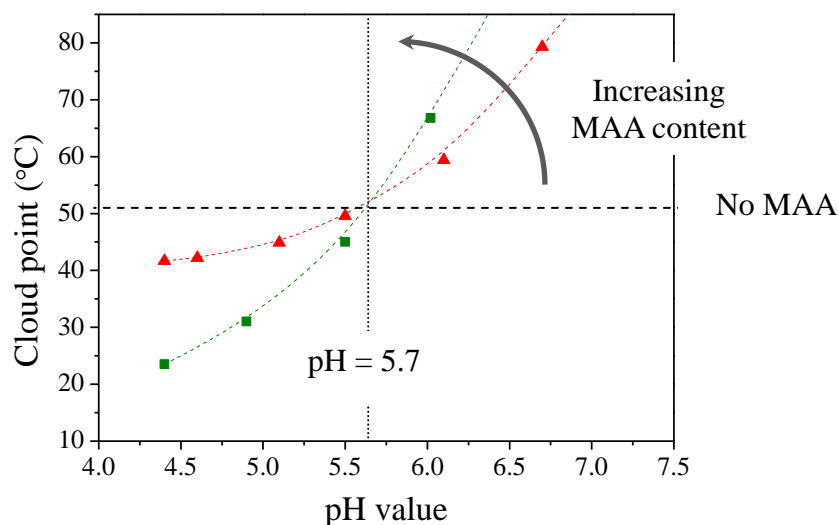


**Figure 5.** Cloud point temperature ( $T_{50\%}$ ) versus pH for 0.5 wt% solutions of Ma0 (0 mol% MAA, ----), Ma1 (14 mol% MAA, ▲) and Ma2 (42 mol% MAA, ■). The dashed lines are guides to eyes.

### 3. Surfactant-free emulsion polymerizations of BMA and S initiated by P(PEOMA<sub>300</sub>-*co*-MAA-*co*-S)-SG1 macroalkoxyamine initiators

Having established the dual pH- and temperature-responsive behavior of the P(PEOMA<sub>300</sub>-*co*-MAA-*co*-S)-SG1 terpolymers, the macroalkoxyamines were next used to initiate the emulsion polymerization of BMA and S in order to form self-assembled amphiphilic block copolymers (Table 3). The reaction temperature was fixed at 85 °C to ensure an efficient control of the polymerization, while we systematically varied the MAA content, the concentration of macroinitiator, and the pH value. Their effect on the polymerization kinetics, on the control over the formation of amphiphilic block copolymers, and on the self-assembled nano-objects stability and morphology was studied.

#### 3.1 Effect of MAA content at pH = 7.5

In order to assess the effect of the MAA content on both the kinetics and the control of the

polymerization, three experiments were carried out at a fixed pH of 7.5 using Ma1 (E2, 14 mol% MAA), Ma2 (E6, 42 mol% MAA) and Ma3 (E8, 68 mol% MAA) (Table 3). As shown above (Figure 5), all three macroalkoxyamine initiators are fully water-soluble under such pH conditions, and do not exhibit any cloud point. They can therefore efficiently contribute to the electrosteric stabilization of the particles. As shown in Figure 6, the polymerization performed with 14 mol% of MAA reached a high, however incomplete, conversion (ca. 75%) within 1.5 h. Limited conversions have already been observed in the literature for NMP polymerizations initiated by macroinitiators based on styrene as a comonomer. They might be explained by an accumulation of SG1 subsequently to irreversible termination reactions at high conversions due to a too low styrene concentration in the suspension medium. In addition, the polymerization rates and the final conversions decreased with increasing MAA content in the copolymer, which is likely due to the concomitant increase of ionic strength (induced by the increased amount of NaOH required to reach pH 7.5), as previously observed for similar emulsion polymerization experiments initiated by P(P<sub>EO</sub>MA<sub>950-co</sub>-S)-SG1.<sup>17</sup> In the present case, it is nevertheless difficult to de-correlate the influence of the macroinitiator architecture from that of the ionic strength, on the conformation in water of the PEO-based macroalkoxyamines. However, it is very likely that the initial state is different between the three experiments, which may impact the activation/deactivation rate constants, and therefore the reaction rate and the final conversion.

The polymerizations carried out using Ma1 or Ma2 as macroinitiators were relatively well controlled as attested by the linear evolution of  $M_n$  as a function of the overall weight conversion (Figure 6b).

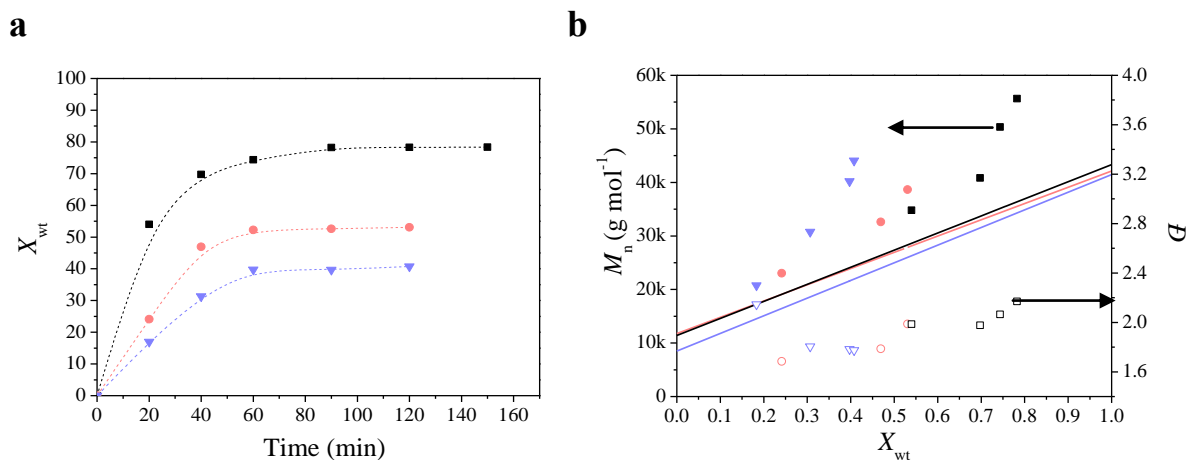


**Figure 6.** Evolutions of: a) monomer weight conversion with time, and b)  $M_n$  (filled symbols) and  $D$  (empty symbols) vs weight conversion during the surfactant-free emulsion polymerization of BMA and S using P(PEOMA<sub>300-co</sub>-MAA-co-S) macroalkoxyamine initiators of increasing MAA molar fractions at pH = 7.5. E2: Ma1 (■, 14 mol% MAA), E6: Ma2 (●, 42 mol% MAA) and E8: Ma3 (▼, 68 mol% MAA) (Table 3). The straight lines in the  $M_n$  vs  $X_{wt}$  plots correspond to the theoretical evolution.

However, as the MAA content increased, the crossover efficiency and the quality of control over chain growth were gradually lost which is once again likely related to the concomitant increase of ionic strength as discussed previously.<sup>17</sup> In addition, a small shoulder on the low molar mass side was observed for Ma2 and Ma3, indicating the presence of dead chains formed by irreversible termination reaction either during the synthesis of the macroalkoxyamine or during the reinitiation step (Figure 7). Although care was taken to stop the reaction at relatively low conversion, fast consumption of styrene during the synthesis of the macroinitiator may have favored such side reactions. The shift of the SEC peaks towards higher molar masses with increasing monomer conversion, nonetheless indicates an efficient reinitiation step and the effective synthesis of amphiphilic block copolymers.

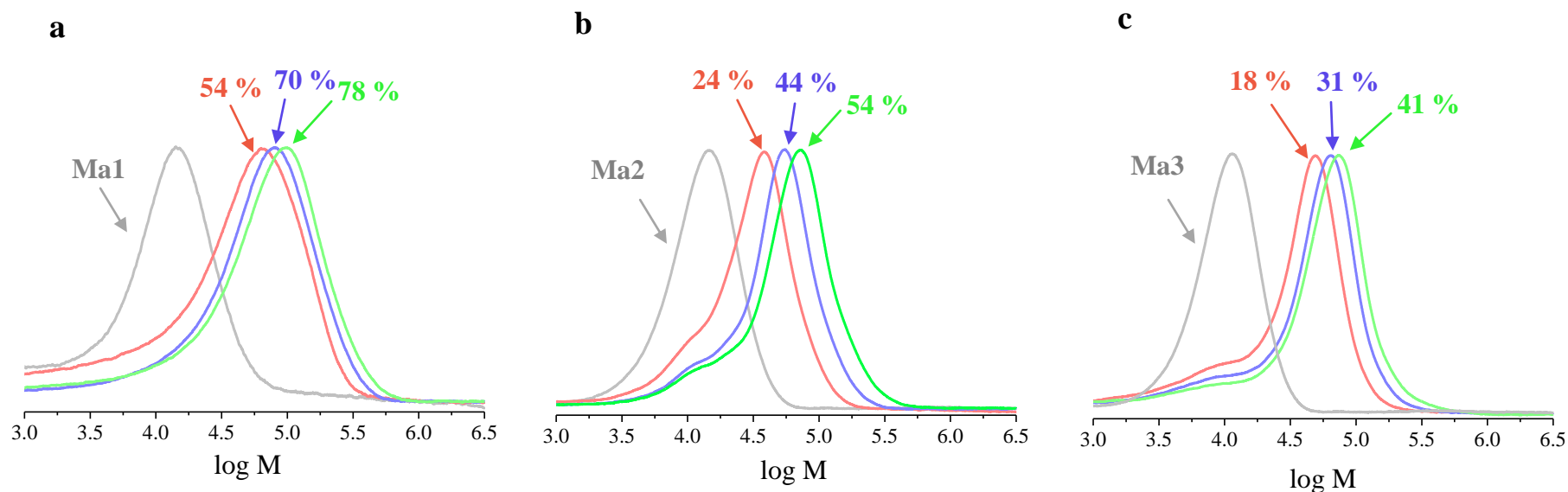


**Figure 7.** Evolution of the size exclusion chromatograms with weight conversion during the surfactant-free emulsion polymerization of BMA and S using P(PEOMA<sub>300-co</sub>-MAA-*co*-S) macroalkoxyamine initiators of increasing MAA molar fractions at pH = 7.5. a) E2: Ma1 (14 mol% MAA), b) E6: Ma2 (42 mol% MAA) and c) E8: Ma3 (68 mol% MAA) (Table 3).

Figure 8 shows the TEM images of the final self-assembled block copolymers particles. All latexes exhibited a good colloidal stability and contained particles of different morphologies as evidenced by TEM. For low MAA contents (E2, 14 mol%), the resulting amphiphilic P(P<sub>EO</sub>MA<sub>300</sub>-*co*-MAA-*co*-S)-*b*-P(BMA-*co*-S) block copolymers self-assembled into a mixture of small spherical particles ( $D_n = 59$  nm,  $D_w/D_n = 1.32$ ), fibers ( $D_n = 65$  nm) and a minor population of vesicles. When the MAA content was increased to 42 mol% (E6), only spherical particles were obtained, which indicates a better stabilization ability of the macroalkoxyamine initiator upon increasing the number of anionic carboxylate groups. The particles diameter was slightly bigger ( $D_n = 78$  nm) and the size distribution narrower ( $D_w/D_n = 1.09$ ). Finally, a mixture of spherical particles ( $D_n = 108$  nm,  $D_w/D_n = 1.06$ ), short rods, fibers and vesicles was obtained when the MAA percentage was increased to 68 mol% (E8). This last result is likely due to a competition between increasing hydrophilicity (upon increasing MAA content) and a salting out effect as the NaOH concentration used to adjust the pH value was increased from 17 to 64 mM when increasing MAA molar fraction from 14 to 68 mol% (Table 3). Similar findings have been reported by Boissé and coworkers for the RAFT-mediated emulsion polymerization of styrene using a pH-sensitive P(AA-*co*-PEOA) stabilizing block.<sup>15</sup> However in this previous work, the macroRAFT agent was not thermoresponsive and a much larger salt concentration (*i.e.* 380 mM) was required to induce a morphological change.

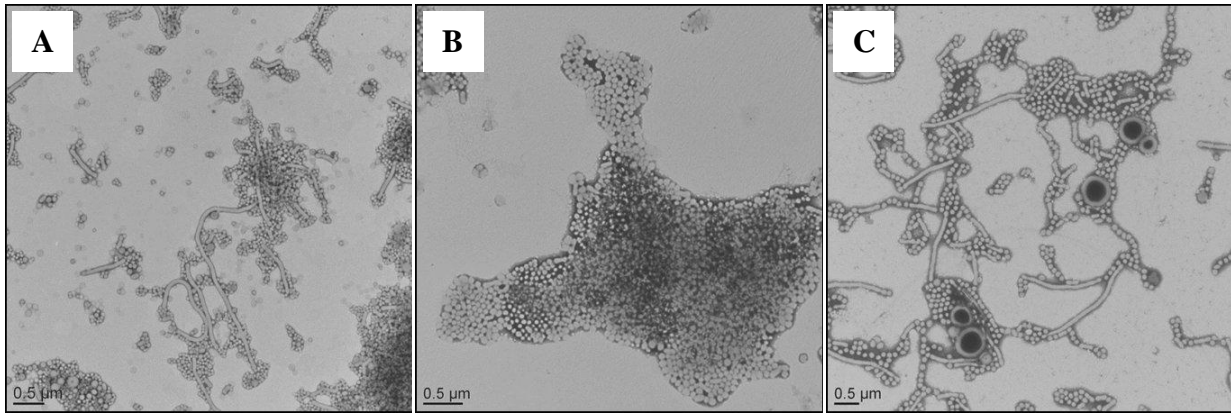


**Figure 8.** TEM images of the final P(PEOMA<sub>300-co</sub>-MAA-*co*-S)-*b*-P(BMA-*co*-S) latex particles obtained by surfactant-free emulsion polymerization of BMA and S using P(PEOMA<sub>300-co</sub>-MAA-*co*-S) macroalkoxyamine initiators of increasing MAA molar fractions at pH = 7.5. A) E2: Ma1 (14 mol% MAA), B) E6: Ma2 (42 mol% MAA) and C) E8: Ma3 (68 mol% MAA) (Table 3).

### 3.2 Effect of pH

To investigate the effect of pH on the emulsion polymerization kinetics, the control over molar mass and on the final morphology of the latex particles, four experiments were conducted at pH = 5.0, 6.0, 7.5 and 9.1, respectively, using Ma2 as macroinitiator (42 mol% MAA, Table 3, E4 to E7). As mentioned earlier, the ionization degree of the MAA subunits in the P(PEOMA<sub>300-co</sub>-MAA-*co*-S)-SG1 macroalkoxyamine initiator is very high at pH = 7.5 and 9.1. Therefore, in such conditions, Ma2 was fully soluble regardless of temperature (Figure 5). However, at low pH (pH = 6.0 and 5.0), the situation was different and the macroalkoxyamine initiator was no longer water-soluble at the reaction temperature. Indeed, according to Figure 5, Ma2 solution was cloudy above 30 °C at pH 5.0 and above 70 °C at pH 6.0.<sup>35</sup>

Figure 9a shows the evolution of the weight conversion vs time for increasing pH values. It

is seen that the polymerization rate increased with decreasing pH with the exception of pH 5.0 for which the reaction rate was unexpectedly low. SG1 is known to degrade in acidic media. Therefore, the free SG1 concentration should decrease with decreasing pH, which should result in higher reaction rates, as observed experimentally from pH 9.1 to pH 6.0. The unexpectedly low polymerization rate at pH 5 is thus likely due to the poor water solubility of Ma2 mentioned above. The decrease in SG1 concentration shifted the NMP equilibrium towards the active species, which also led to more irreversible termination reactions resulting in limiting conversions.

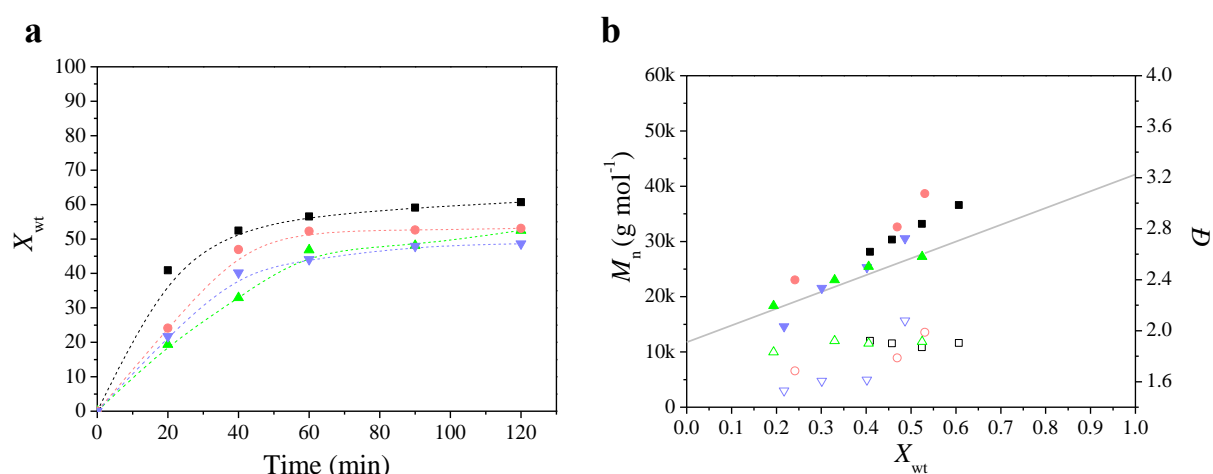


**Figure 9.** Evolutions of: a) monomer weight conversion with time, and b)  $M_n$  (filled symbols) and  $\mathcal{D}$  (empty symbols) vs weight conversion during the surfactant-free emulsion polymerization of BMA and S using the Ma2 macroalkoxyamine initiator (42 mol% MAA) for increasing pH values. E4: pH = 5.0 ( $\blacktriangle$ ); E5: pH = 6.0 ( $\blacksquare$ ); E6: pH = 7.5 ( $\bullet$ ) and E7: pH = 9.1 ( $\blacktriangledown$ ) (Table 3). The straight lines in the  $M_n$  vs  $X_{wt}$  plots correspond to the theoretical evolution.

Figure 9b and Table 3 show that the pH did not affect the evolution of  $M_n$  with conversion and the initiation efficiency to a significant extent. On the other hand, the TEM images of

Figure 10 clearly show that the particles morphology evolved from mainly vesicles at pH = 5.0, to a mixture of fibers and vesicles with a minor population of very small spherical particles at pH = 6.0, to mainly spheres around pH = 7.5 ( $D_n = 78$  nm and  $D_w/D_n = 1.09$ ), and finally smaller spheres at higher pH ( $D_n = 70$  nm and  $D_w/D_n = 1.07$ , pH = 9.1). This morphological evolution shows that as expected, the stabilization efficiency of the macroalkoxyamine initiator increases with increasing the degree of ionization of MAA.

It is worth emphasizing here that the P(PEOMA<sub>950-co-S</sub>)-SG1 macroinitiator reported in our previous article (with longer pendant PEO chains and without MAA units) produced exclusively spherical particles at low pH values under similar conditions, whereas increasing pH favored the formation of fibers and vesicles.<sup>17</sup> The above results thus clearly demonstrate that the morphology of block copolymers obtained by PISA closely depends on the nature of the hydrophilic block, and that is possible to reverse the sequence order (with the formation of vesicles at low pH and spheres at higher pH), by using a thermoresponsive hydrophilic block whose LCST can be finely tuned in response to a change of pH, while maintaining a fixed composition and degree of polymerization of the hydrophobic block. More surprising was the stability of the latex suspensions above the cloud point of the macroalkoxyamine initiators at pH 5.0 and 6.0. During polymerization, the medium suddenly became milky when the temperature reached the cloud point temperature but the colloidal stability was maintained during and after polymerization (Figure S3, Supporting Information). In this regard, it should be reminded that the emulsion was broken in a short period of time when P(PEOMA<sub>300-co-S</sub>)-SG1 (without MAA subunits) was used as macroinitiator under similar conditions.<sup>17</sup> This points to the determinant role of MAA in imparting colloidal stability to the formed latex particles even for reaction temperatures exceeding cloud points.

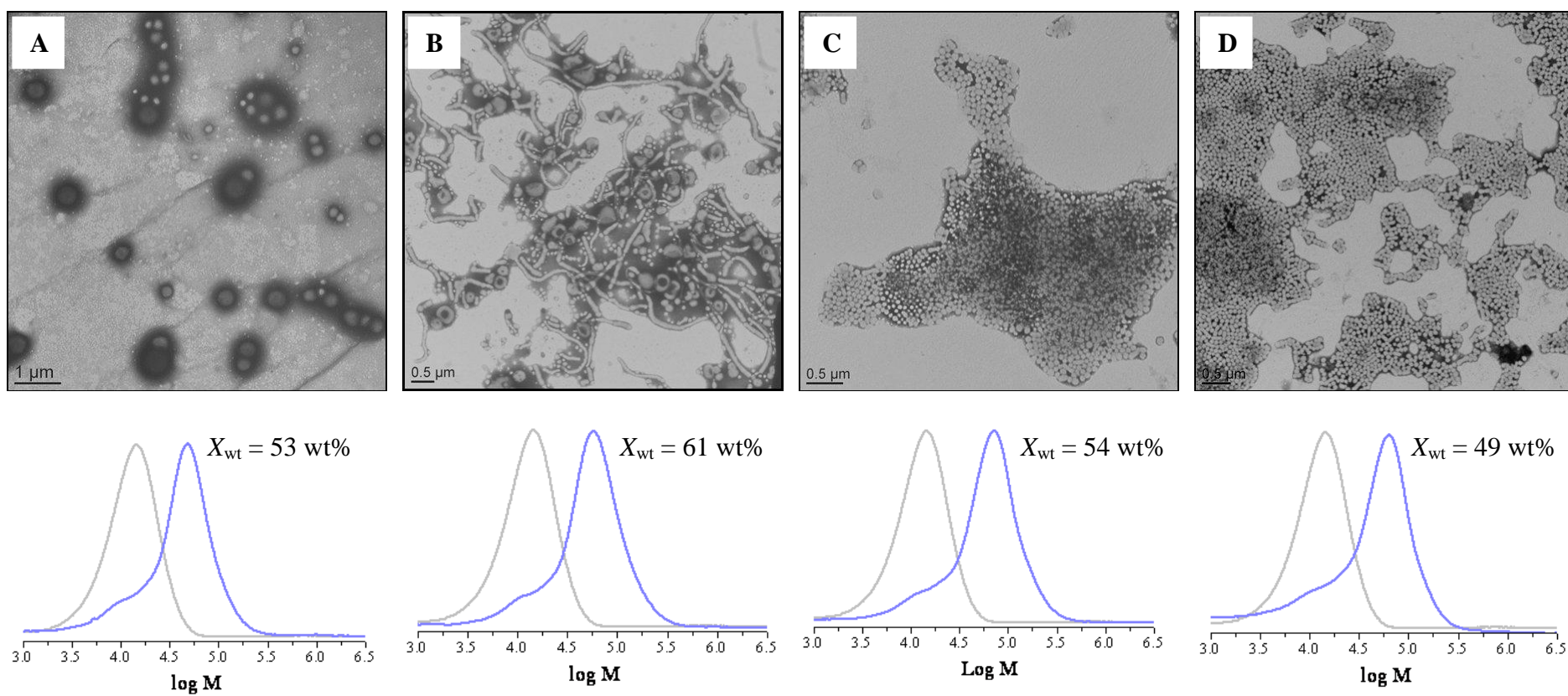


**Figure 10.** Evolution of the size exclusion chromatograms and TEM images of the final P(PEOMA<sub>300</sub>-co-MAA-co-S)-b-P(BMA-co-S) latex particles obtained by surfactant-free emulsion polymerization of BMA and S using the Ma2 macroalkoxyamine initiator (42 mol% MAA) for increasing pH values. A: E4, pH = 5.0; B: E5, pH = 6.0; C: E6, pH = 7.5 and D: E7, pH = 9.1. See Table 3 for detailed experimental conditions.

Indeed, around pH 5-6, it is expected that only a fraction of the MAA units is protonated. The resulting self-assembled morphologies are therefore likely stabilized by the presence of residual carboxylate anions. The fact that the terpolymers exhibit a cloud point at relatively high pH values is thus essential in the context of this work as this guarantees that the higher order morphologies formed under such conditions are stabilized by electrosteric repulsions. In the present system, such a fine control can only be achieved by the addition of hydrophobic units (S in the present case). Indeed, it has been reported earlier that P(PEOMA<sub>300</sub>-*co*-MAA) copolymers similar to the terpolymers reported here but without S units, did not display any cloud point above pH 5.<sup>32</sup> It was shown that the cloud point dropped by around 1 °C per mole of hydrophobic monomer which is a typical behavior of thermoresponsive polymers. It is perhaps also worth mentioning that the latex suspensions did not exhibit any change of viscosity on visual inspection, either in the course of polymerization at high temperature or on cooling to room temperature, suggesting that no post-polymerization order-order morphological transitions had occurred in our system. Actually until now, stimuli-induced morphological transitions have only been observed for solvent-based formulations or aqueous RAFT dispersion polymerization, and have never been reported for RAFT aqueous emulsion polymerization.<sup>1,2</sup>

### *3.3 Effect of macroinitiator concentration*

The effect of the macroinitiator concentration was studied using Ma1 at a fixed pH value of 7.5 (E1 to E3 in Table 3). The initial concentration of Ma1 was varied from 2.6 mM to 9.0 mM, while the overall amount and composition of the hydrophobic monomers (BMA and S) remained unchanged. As shown in Figure 11a, the polymerization kinetics curves were strongly dependent on the initiator concentration, the highest reaction rate being obtained for the highest concentration. This result is similar to that previously observed in the emulsion

polymerization of methyl methacrylate with a small proportion of styrene initiated by a water soluble P(MAA-*co*-sodium 4-styrene sulfonate) macroalkoxyamine,<sup>36</sup> or in our previous study involving P(PEOMA<sub>950</sub>-*co*-S)-SG1 as macroinitiator.<sup>17</sup> It can be interpreted as being the direct consequence of the persistent radical effect and of the proportion of SG1 released in the medium with respect to the initial macroalkoxyamine concentration, which is expected to be less important when the later concentration increases, hence providing more propagating chains.<sup>37</sup> Figure 11b shows that the experimental  $M_n$  increased linearly with monomer conversion, even though they did not fit with the predicted values, which is due to the use of PMMA standards. Furthermore, the shift of the SEC traces towards higher molar masses at full conversion (see Figure S4, Supporting Information) illustrates the controlled growth of the hydrophobic block with the formation of amphiphilic block copolymers. A small shoulder was however observed on the low mass side for the highest Ma1 concentration (E3), indicating the presence of unreacted (and likely dead) Ma1 chains. In most cases, there was also a shoulder on the high molar mass side. For all these reasons, the final molar mass distributions were quite broad ( $1.9 < \mathcal{D} < 2.2$ ).

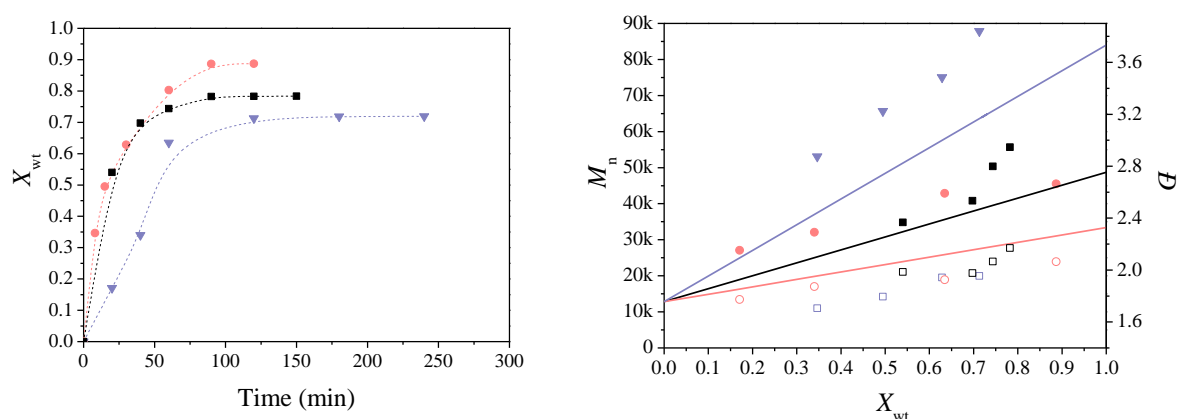


**Figure 11.** Evolutions of: a) monomer weight conversion with time and b)  $M_n$  and  $\mathcal{D}$  vs. weight conversion during the surfactant-free emulsion polymerization of BMA and S using increasing Ma1 concentrations at pH 7.5. E1: 2.6 mM ( $\blacktriangledown$ ), E2: 5.2 mM ( $\blacksquare$ ) and E3: 9.1 mM ( $\bullet$ ) (Table 3). The straight lines in the  $M_n$  vs  $X_{wt}$  plots correspond to the theoretical evolution.

In all experiments, stable amphiphilic P(PEOMA<sub>300-co</sub>-MAA-co-S)-*b*-P(BMA-co-S) diblock copolymers were formed that self-assembled during the emulsion polymerization reaction. Figure 12 shows the cryo-TEM pictures of the different latexes obtained. A clear relationship between the Ma1 concentration (and therefore the length of the core-forming block) and the final particle morphology was observed. The final latex suspension was predominantly composed of spheres and fibers for 9.1 mM (E3), a mixture of spheres, fibers and vesicles for 5.2 mM (E2) and vesicles for 2.6 mM (E1). The morphology of the self-assembled copolymers therefore evolved from spheres to worms to vesicles with increasing the molar mass of the hydrophobic block. This morphological evolution is similar to previous findings in the literature and is typical of block copolymers self-assembly via the PISA mechanism using NMP<sup>38,39</sup> or RAFT.<sup>15,35,40,41,42,43</sup> However, it is worth pointing out here that the polymerization performed under the same conditions as E1 (see Table 3), but using P(PEOMA<sub>950-co</sub>-S)-SG1 as macroinitiator, led to an unstable latex,<sup>17</sup> highlighting once again the determinant role of MAA in controlling the solvation properties of the hydrophilic block, not only for low pH values, when the reaction temperature is well above the LCST of the stabilizer block, but also at higher pHs, when the polymerization temperature is lower than the LCST. Indeed, the macroinitiator is then fully ionized, which significantly improves the stability of the self-assembled block copolymers particles.

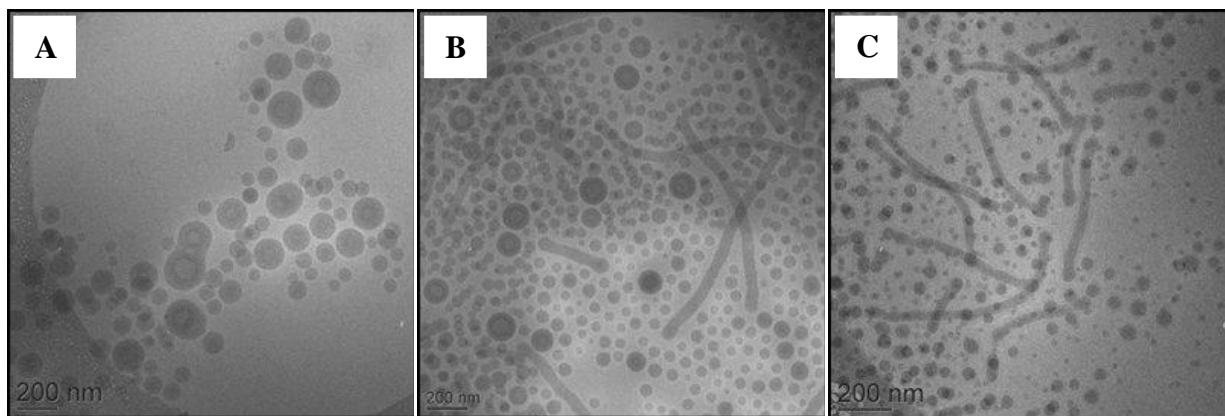


**Figure 12.** Cryo-TEM images of the final P(PEOMA<sub>300-co</sub>-MAA-*co*-S)-*b*-P(BMA-*co*-S) latex particles obtained by surfactant-free emulsion polymerization of BMA and S using increasing MaI concentrations at pH 7.5. A) E1: 2.6 mM, B) E2: 5.2 mM and C) E3: 9.1 mM (Table 3).

#### 4. Block copolymers self-assembly in the presence of silica particles

Taking advantage of the well-known affinity of PEO-based polymers for silica surfaces, we recently demonstrated the successful synthesis of silica/polymer hybrid particles through nitroxide-mediated emulsion polymerization of BMA and S using P(PEOMA<sub>950-co</sub>-S)-SG1 as macroinitiator.<sup>44</sup> Adsorption of the macroalkoxyamine initiator at the silica surface enabled the polymerization to be confined to the interface resulting in a variety of particle morphologies, which were function of the pH and the silica particle size.<sup>45</sup> Following a similar strategy using macromolecular RAFT (macroRAFT) agents instead of macroalkoxyamine initiators, several reports have highlighted the importance of the composition of the controlling agent on the morphology of the hybrid particles. In particular, the incorporation of hydrophobic monomer units into the macroRAFT copolymers was shown to be a key requirement for the successful formation of polymer-encapsulated inorganic particles.<sup>46,47</sup> Following this idea, we aimed in the present work to increase the

hydrophobic character of the P(P<sub>EO</sub>MA<sub>300</sub>-*co*-MAA-*co*-S) macroinitiators by decreasing the suspension pH, in order to promote the formation of an encapsulating shell in the subsequent emulsion polymerization reaction. In order to favor macroalkoxyamine adsorption on the silica surface for a wide range of pH values, Ma1 was selected as macroinitiator as it contained the least number of MAA units. Three emulsion polymerization experiments were then carried out in the presence of 77 nm diameter silica particles (Figure S5, Supporting Information) at a fixed concentration of 50 g L<sup>-1</sup> and three different pH values (pH = 6.0, 7.5 and 9.0), corresponding to cloud point temperatures respectively below, close to, and above the reaction temperature (*i.e.* 85 °C, see Figure 5). In the three cases, the SEC trace of the macroinitiator was clearly shifted toward higher molar masses indicating the successful formation of block copolymers, with however the presence of unreacted macroinitiator as attested by the small peak in the low molar mass region of the chromatograms (Figure S6, Supporting Information).

In order to avoid any drying artifact that can occur during sample preparation by conventional TEM, making it difficult to properly interpret the data, the final composite particles were observed by cryo-TEM (Figure 13). All composite particles have a multipod-like structure regardless of experimental conditions. At pH = 6.0 (Figures 13A and 13B), the silica spheres (in dark) are surrounded by in average one or two polymer nodules (in grey). A few silica-decorated vesicles and/or fibers can also be seen in agreement with the previous observations in the absence of silica. One can also notice the presence of free silica particles devoid of polymer nodules at their surface and of free latex particles suggesting only moderate affinity between the two populations of particles. At pH = 7.5 (Figures 13C and 13D), the silica spheres are surrounded by in average 3 or 4 polymer particles irregularly distributed all around the inorganic core, and each silica particle has at least one polymer nodule attached to its surface (*i.e.* there is no free silica). Some of the polymer nodules have

coalesced with neighboring latex particles in solution to form short rods lying adjacent to the silica beads (white circles). Figures 13E and 13F show that an even greater number of polymer nodules are present on the silica surface when the pH is further increased to 9.0. Remarkably enough, the obtained structures present multiple protruding short worms that are extending radially from the inorganic surface in a sea urchin-like morphology (yellow circles). The worms are composed of at most two or three partially coalesced latex particles and are most often seen together with spherical nodules. Such an unconventional morphology is obviously a direct consequence of the dual pH/temperature sensitive properties of the macroinitiator. Indeed, the P(PEOMA<sub>950-co-S</sub>)-SG1 macroalkoxyamine mainly led to hemi-capped or core-shell particles under the same conditions.<sup>44</sup> One possible explanation that might be put forward for such morphology is the presence of ionized MAA units in the stabilizer block. These ionic groups would create charge repulsions between neighboring worms and with the negatively charged silica surface, which would prevent the particles to come close to each other, and to lie flat on the inorganic surface in order to minimize the total interfacial energy. The higher affinity of the self-assembled block copolymers for the silica surface at pH 9 was not expected. Indeed, according to the literature, macroinitiator adsorption should decrease with increasing pH as the number of silanol groups decreases. The presence of ionized MAA units at pH 9 should further lower adsorption by electrostatic repulsions. However, the Ma1 macroinitiator has a LCST of around 58 °C at pH 6 (see Figure 5), and the polymer chains are therefore collapsed at the reaction temperature, with the ionized MAA groups likely located at the polymer/water interface. Such a conformation may not favor adsorption. As a matter of fact, above the LCST, the affinity between the polymer segments is likely greater than that between the EO units and the silanol groups, hindering adsorption while the carboxylate anions add additional electrostatic repulsions. At pH 9 on the contrary, the comb-like copolymer exhibits a fully extended chain conformation,

promoting adsorption.

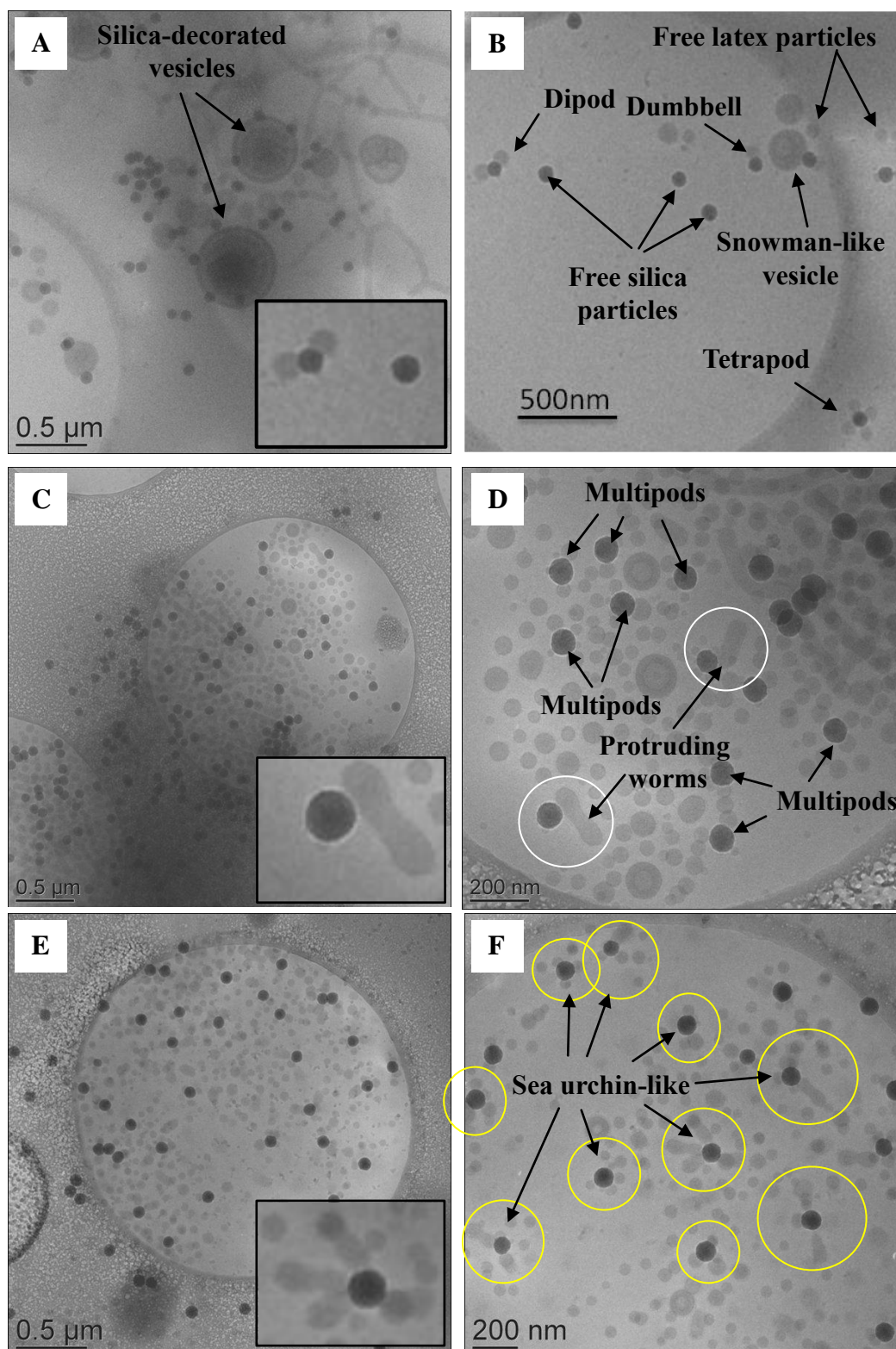


**Figure 13.** Cryo-TEM images of the hybrid latex particles obtained by surfactant-free emulsion polymerization of BMA and S in the presence of 77 nm diameter silica particles using Ma 1 ( $5.2 \text{ mmol L}^{-1}$ , see Table 2 and 3 for details) as macroinitiator for different pH

values. (A, B) ES01, pH = 6.0, (C, D) ES02 pH = 7.5 and (E, F) ES03, pH = 9.0.

## CONCLUSIONS

Comb-like P(P<sub>EO</sub>MA<sub>300-co</sub>-MAA-co-S)-SG1 macroalkoxyamine terpolymer initiators with dual pH/temperature responsive behavior were synthesized by NMP, and used to control the emulsion polymerization of BMA with a small proportion of styrene. The cloud points of the terpolymers could be fine-tuned over a large range of temperatures from 20 to 90 °C by varying the suspension pH or the copolymer composition. Such changes in solution properties of the stabilizer block had a drastic influence on the morphology of the final particles. The polymerization carried out at pH 5.0 for a fixed MAA molar fraction of 42 %, resulted in a majority of vesicles which did not reorganize into fibers or spheres on cooling to room temperature, whereas P(P<sub>EO</sub>MA<sub>950-co</sub>-S)-SG1 exclusively led to spherical particles under the same conditions. Increasing the suspension pH from 5.0 to 9.1 favored the formation of fibers and spherical micelles, whose morphologies were promoted by an increase of the interfacial curvature as the degree of ionization of the MAA units increased. Similarly, varying the macroinitiator concentration, and hence the degree of polymerization of the core-forming block at a fixed pH of 7.5 enabled to target a majority of vesicles, which can again be explained by geometric considerations. Interestingly, all latex suspensions were stable during and after polymerization, even when the stabilizer block was in the collapsed state (*i.e.* when the polymerization temperature was higher than its LCST). This was attributed to the presence of ionized MAA units. Compared to their P(P<sub>EO</sub>MA<sub>950-co</sub>-S)-SG1 homologues, the incorporation of only 14 mol% of MAA in the terpolymers was enough to induce a drastic change in particle morphology. When the MAA content was increased to 68 mol%, the terpolymer was no longer thermoresponsive, and behaved more like a pH-sensitive

stabilizer. At last, the polymerization conducted in the presence of colloidal silica using the 14 mol% MAA terpolymer, led to the formation of polymer worms radially expanding from the silica core in a sea urchin-like morphology. This morphology is presumably governed by a complex interplay between attractive forces allowing the macroinitiator to adsorb on the silica surface and repulsive electrostatic forces between the growing self-assembled block copolymers. The mechanism of formation of such sea urchin-like particles is however not yet fully understood and will clearly warrant further investigations.

## ACKNOWLEDGMENTS

The financial support from the China Scholarship Council is greatly acknowledged. The authors would like to thank Olivier Boyron (C2P2) for his help concerning SEC analyses. Arkema is thanked for kindly providing the BlockBuilder® initiator and the SG1 nitroxide used in this work.

## REFERENCES

1. Rieger, J., Guidelines for the Synthesis of Block Copolymer Particles of Various Morphologies by Raft Dispersion Polymerization. *Macromol. Rapid Commun.* **2015**, *36*, 1458-1471.
2. Canning, S. L.; Smith, G. N.; Armes, S. P., A Critical Appraisal of Raft-Mediated Polymerization-Induced Self-Assembly. *Macromolecules* **2016**, *49*, 1985-2001.
3. Lansalot, M.; Rieger, J.; D'Agosto, F., Polymerization-Induced Self-Assembly: The Contribution of Controlled Radical Polymerization to the Formation of Self-Stabilized Polymer Particles of Various Morphologies. In *Macromolecular Self-Assembly*, John Wiley & Sons, Inc.: 2016; pp 33-82.
4. Save, M.; Guillaeneuf, Y.; Gilbert, R. G., Controlled Radical Polymerization in

Aqueous Dispersed Media. *Aust. J. Chem.* **2006**, *59*, 693-711.

5. Zetterlund, P. B.; Thickett, S. C.; Perrier, S.; Bourgeat-Lami, E.; Lansalot, M., Controlled/Living Radical Polymerization in Dispersed Systems: An Update. *Chem. Rev.* **2015**, *115*, 9745-800.
6. Qiu, Q.; Liu, G.; An, Z., Efficient and Versatile Synthesis of Star Polymers in Water and Their Use as Emulsifiers. *Chem. Commun.* **2011**, *47*, 12685-12687.
7. Thompson, K. L.; Mable, C. J.; Cockram, A.; Warren, N. J.; Cunningham, V. J.; Jones, E. R.; Verber, R.; Armes, S. P., Are Block Copolymer Worms More Effective Pickering Emulsifiers Than Block Copolymer Spheres? *Soft Matter* **2014**, *10*, 8615-8626.
8. Chenal, M.; Rieger, J.; Véchambre, C.; Chenal, J.-M.; Chazeau, L.; Creton, C.; Bouteiller, L., Soft Nanostructured Films with an Ultra-Low Volume Fraction of Percolating Hard Phase. *Macromol. Rapid Commun.* **2013**, *34*, 1524-1529.
9. Cenacchi-Pereira, A. G., E.; D'Agosto, F.; Lansalot, M.; Bourgeat-Lami, E., Encapsulation with the Use of Controlled Radical Polymerization. In *Encyclopedia of Polymeric Nanomaterials*, Kobayashi, S.; Müllen, K., Eds. Springer-Verlag Berlin Heidelberg, 2015.
10. Bourgeat-Lami, E.; D'Agosto, F.; Lansalot, M., Synthesis of Nanocapsules and Polymer/Inorganic Nanoparticles through Controlled Radical Polymerization at and near Interfaces in Heterogeneous Media. *Adv. Polym. Sci.* **2016**, *270*, 123-161.
11. Israelachvili, J. N.; Mitchell, D. J.; Ninham, B. W., Theory of Self-Assembly of Hydrocarbon Amphiphiles into Micelles and Bilayers. *J. Chem. Soc., Faraday Trans. 2* **1976**, *72*, 1525-1568.
12. Blanz, A.; Armes, S. P.; Ryan, A. J., Self-Assembled Block Copolymer Aggregates: From Micelles to Vesicles and Their Biological Applications. *Macromol. Rapid Commun.* **2009**, *30*, 267-277.

13. Blanazs, A.; Ryan, A. J.; Armes, S. P., Predictive Phase Diagrams for Raft Aqueous Dispersion Polymerization: Effect of Block Copolymer Composition, Molecular Weight, and Copolymer Concentration. *Macromolecules* **2012**, *45*, 5099-5107.
14. Lesage de la Haye, J.; Zhang, X.; Chaduc, I.; Brunel, F.; Lansalot, M.; D'Agosto, F., The Effect of Hydrophile Topology in Raft-Mediated Polymerization-Induced Self-Assembly. *Angew. Chem. Int. Ed.* **2016**, *55*, 3739-3743.
15. Boisse, S.; Rieger, J.; Belal, K.; Di-Cicco, A.; Beaunier, P.; Li, M.-H.; Charleux, B., Amphiphilic Block Copolymer Nano-Fibers Via Raft-Mediated Polymerization in Aqueous Dispersed System. *Chem. Commun.* **2010**, *46*, 1950-1952.
16. Zhang, L.; Eisenberg, A., Morphogenic Effect of Added Ions on Crew-Cut Aggregates of Polystyrene-B-Poly(Acrylic Acid) Block Copolymers in Solutions. *Macromolecules* **1996**, *29*, 8805-8815.
17. Qiao, X. G.; Lansalot, M.; Bourgeat-Lami, E.; Charleux, B., Nitroxide-Mediated Polymerization-Induced Self-Assembly of Poly(Poly(Ethylene Oxide) Methyl Ether Methacrylate-Co-Styrene)-B-Poly(N-Butyl Methacrylate-Co-Styrene) Amphiphilic Block Copolymers. *Macromolecules* **2013**, *46*, 4285-4295.
18. Sanson, N.; Rieger, J., Synthesis of Nanogels/Microgels by Conventional and Controlled Radical Crosslinking Copolymerization. *Polym. Chem.* **2010**, *1*, 965-977.
19. Blanazs, A.; Verber, R.; Mykhaylyk, O. O.; Ryan, A. J.; Heath, J. Z.; Douglas, C. W. I.; Armes, S. P., Sterilizable Gels from Thermoresponsive Block Copolymer Worms. *J. Am. Chem. Soc.* **2012**, *134*, 9741-9748.
20. Warren, N. J.; Mykhaylyk, O. O.; Mahmood, D.; Ryan, A. J.; Armes, S. P., Raft Aqueous Dispersion Polymerization Yields Poly(Ethylene Glycol)-Based Diblock Copolymer Nano-Objects with Predictable Single Phase Morphologies. *J. Am. Chem. Soc.* **2014**, *136*, 1023-1033.

21. Lovett, J. R.; Warren, N. J.; Ratcliffe, L. P. D.; Kocik, M. K.; Armes, S. P., Ph-Responsive Non-Ionic Diblock Copolymers: Ionization of Carboxylic Acid End-Groups Induces an Order–Order Morphological Transition. *Angew. Chem. Int. Ed.* **2015**, *54*, 1279-1283.
22. Penfold, N. J. W.; Lovett, J. R.; Warren, N. J.; Verstraete, P.; Smets, J.; Armes, S. P., Ph-Responsive Non-Ionic Diblock Copolymers: Protonation of a Morpholine End-Group Induces an Order-Order Transition. *Polym. Chem.* **2016**, *7*, 79-88.
23. Penfold, N. J. W.; Lovett, J. R.; Verstraete, P.; Smets, J.; Armes, S. P., Stimulus-Responsive Non-Ionic Diblock Copolymers: Protonation of a Tertiary Amine End-Group Induces Vesicle-to-Worm or Vesicle-to-Sphere Transitions. *Polym. Chem.* **2017**, *8*, 272-282.
24. Figg, C. A.; Simula, A.; Gebre, K. A.; Tucker, B. S.; Haddleton, D. M.; Sumerlin, B. S., Polymerization-Induced Thermal Self-Assembly (Pitsa). *Chem. Sci.* **2015**, *6*, 1230-1236.
25. Delaittre, G.; Save, M.; Charleux, B., Nitroxide-Mediated Aqueous Dispersion Polymerization: From Water-Soluble Macroalkoxyamine to Thermosensitive Nanogels. *Macromol. Rapid Commun.* **2007**, *28*, 1528-1533.
26. Jia, Z.; Bobrin, V. A.; Truong, N. P.; Gillard, M.; Monteiro, M. J., Multifunctional Nanoworms and Nanorods through a One-Step Aqueous Dispersion Polymerization. *J. Am. Chem. Soc.* **2014**, *136*, 5824-5827.
27. Truong, N. P.; Whittaker, M. R.; Anastasaki, A.; Haddleton, D. M.; Quinn, J. F.; Davis, T. P., Facile Production of Nanoaggregates with Tuneable Morphologies from Thermoresponsive P(Degma-Co-Hpma). *Polym. Chem.* **2016**, *7*, 430-440.
28. Hashimoto, N.; Aoyama, T.; Shioiri, T., New Methods and Reagents in Organic Synthesis. 14. A Simple Efficient Preparation of Methyl Esters with Trimethylsilyldiazomethane (Tmschn<sub>2</sub>) and Its Application to Gas Chromatographic Analysis of Fatty Acids. *Chem. Pharm. Bull.* **1981**, *29*, 1475-1478.

29. Nicolas, J.; Dire, C.; Mueller, L.; Belleney, J.; Charleux, B.; Marque, S. R. A.; Bertin, D.; Magnet, S.; Couvreur, L., Living Character of Polymer Chains Prepared Via Nitroxide-Mediated Controlled Free-Radical Polymerization of Methyl Methacrylate in the Presence of a Small Amount of Styrene at Low Temperature. *Macromolecules* **2006**, *39*, 8274-8282.
30. Becer, C. R.; Hahn, S.; Fijten, M. W. M.; Thijs, H. M. L.; Hoogenboom, R.; Schubert, U. S., Libraries of Methacrylic Acid and Oligo(Ethylene Glycol) Methacrylate Copolymers with Lcst Behavior. *J. Polym. Sci. Part A: Polym. Chem.* **2008**, *46*, 7138-7147.
31. Fournier, D.; Hoogenboom, R.; Thijs, H. M. L.; Paulus, R. M.; Schubert, U. S., Tunable Ph- and Temperature-Sensitive Copolymer Libraries by Reversible Addition-Fragmentation Chain Transfer Copolymerizations of Methacrylates. *Macromolecules* **2007**, *40*, 915-920.
32. Jones, J. A.; Novo, N.; Flagler, K.; Pagnucco, C. D.; Carew, S.; Cheong, C.; Kong, X. Z.; Burke, N. A. D.; Stöver, H. D. H., Thermoresponsive Copolymers of Methacrylic Acid and Poly(Ethylene Glycol) Methyl Ether Methacrylate. *J. Polym. Sci. Part A: Polym. Chem.* **2005**, *43*, 6095-6104.
33. Bekturov, E. A.; Bimendina, L. A., Interpolymer Complexes. In *Speciality Polymers*, Springer Berlin Heidelberg: Berlin, Heidelberg, 1981; pp 99-147.
34. Holappa, S.; Kantonen, L.; Winnik, F. M.; Tenhu, H., Self-Complexation of Poly(Ethylene Oxide)-Block-Poly(Methacrylic Acid) Studied by Fluorescence Spectroscopy. *Macromolecules* **2004**, *37*, 7008-7018.
35. Zhang, W.; D'Agosto, F.; Boyron, O.; Rieger, J.; Charleux, B., Toward a Better Understanding of the Parameters That Lead to the Formation of Nonspherical Polystyrene Particles Via Raft-Mediated One-Pot Aqueous Emulsion Polymerization. *Macromolecules* **2012**, *45*, 4075-4084.
36. Brusseau, S.; D'Agosto, F.; Magnet, S.; Couvreur, L.; Chamignon, C.; Charleux, B.,

Nitroxide-Mediated Copolymerization of Methacrylic Acid and Sodium 4-Styrenesulfonate in Water Solution and One-Pot Synthesis of Amphiphilic Block Copolymer Nanoparticles. *Macromolecules* **2011**, *44*, 5590-5598.

37. Fischer, H., The Persistent Radical Effect: A Principle for Selective Radical Reactions and Living Radical Polymerizations. *Chem. Rev.* **2001**, *101*, 3581-3610.

38. Delaittre, G.; Dire, C.; Rieger, J.; Putaux, J.-L.; Charleux, B., Formation of Polymer Vesicles by Simultaneous Chain Growth and Self-Assembly of Amphiphilic Block Copolymers. *Chem. Commun.* **2009**, 2887-2889.

39. Groison, E.; Brusseau, S.; D'Agosto, F.; Magnet, S.; Inoubli, R.; Couvreur, L.; Charleux, B., Well-Defined Amphiphilic Block Copolymer Nanoobjects Via Nitroxide-Mediated Emulsion Polymerization. *ACS Macro Lett.* **2011**, *1*, 47-51.

40. An, Z.; Shi, Q.; Tang, W.; Tsung, C.-K.; Hawker, C. J.; Stucky, G. D., Facile Raft Precipitation Polymerization for the Microwave-Assisted Synthesis of Well-Defined, Double Hydrophilic Block Copolymers and Nanostructured Hydrogels. *J. Am. Chem. Soc.* **2007**, *129*, 14493-14499.

41. Rieger, J.; Grazon, C.; Charleux, B.; Alaimo, D.; Jérôme, C., Pegylated Thermally Responsive Block Copolymer Micelles and Nanogels Via in Situ Raft Aqueous Dispersion Polymerization. *J. Polym. Sci. Part A: Polym. Chem.* **2009**, *47*, 2373-2390.

42. Sugihara, S.; Blanazs, A.; Armes, S. P.; Ryan, A. J.; Lewis, A. L., Aqueous Dispersion Polymerization: A New Paradigm for in Situ Block Copolymer Self-Assembly in Concentrated Solution. *J. Am. Chem. Soc.* **2011**, *133*, 15707-15713.

43. Blanazs, A.; Madsen, J.; Battaglia, G.; Ryan, A. J.; Armes, S. P., Mechanistic Insights for Block Copolymer Morphologies: How Do Worms Form Vesicles? *J. Am. Chem. Soc.* **2011**, *133*, 16581-16587.

44. Qiao, X. G.; Dugas, P. Y.; Charleux, B.; Lansalot, M.; Bourgeat-Lami, E., Synthesis of

Multipod-Like Silica/Polymer Latex Particles Via Nitroxide-Mediated Polymerization-Induced Self-Assembly of Amphiphilic Block Copolymers. *Macromolecules* **2015**, *48*, 545-556.

45. Qiao, X. G.; Lambert, O.; Taveau, J. C.; Dugas, P. Y.; Charleux, B.; Lansalot, M.; Bourgeat-Lami, E., Nitroxide-Mediated Polymerization-Induced Self-Assembly of Block Copolymers at the Surface of Silica Particles: Toward New Hybrid Morphologies. *Macromolecules* **2017**, *50*, 3796-3806.

46. Zgheib, N.; Putaux, J.-L.; Thill, A.; Bourgeat-Lami, E.; D'Agosto, F.; Lansalot, M., Cerium Oxide Encapsulation by Emulsion Polymerization Using Hydrophilic Macroraft Agents. *Polym. Chem.* **2013**, *4*, 607-614.

47. Bourgeat-Lami, E.; França, A. J. P. G.; Chaparro, T. C.; Silva, R. D.; Dugas, P. Y.; Alves, G. M.; Santos, A. M., Synthesis of Polymer/Silica Hybrid Latexes by Surfactant-Free Raft-Mediated Emulsion Polymerization. *Macromolecules* **2016**, *49*, 4431-4440.